Journal of Experimental Botany, Vol. 76, No. 4 pp. 1244–1265, 2025
https://doi.org/10.1093/jxb/erae456 Advance Access Publication 10 November 2024

RESEARCH PAPER

Date palm diverts organic solutes for root osmotic adjustment and protects leaves from oxidative damage in early drought acclimation

Bastian L. Franzisky[1,*], Heike M. Mueller[2], Baoguo Du[3,4,*], Thomas Lux[5], Philip J. White[6,†], Sebastien Christian Carpentier[7,8], Jana Barbro Winkler[9], Joerg-Peter Schnitzler[9], Jörg Kudla[10], Jaakko Kangasjärvi[11,‡], Michael Reichelt[12], Axel Mithöfer[13], Klaus F.X. Mayer[5], Heinz Rennenberg[4], Peter Ache[2], Rainer Hedrich[2], Maxim Messerer[5,*], and Christoph-Martin Geilfus[1]

[1] Department of Soil Science and Plant Nutrition, Hochschule Geisenheim University, D-65366 Geisenheim, Germany
[2] Institute for Molecular Plant Physiology and Biophysics, Biocenter, University Würzburg, D-97082 Würzburg, Germany
[3] College of Life Science and Biotechnology, Mianyang Normal University, Mianxing Road West 166, Mianyang 621000, China
[4] Chair of Tree Physiology, Institute of Forest Sciences, Albert-Ludwigs-Universität Freiburg, Georges-Köhler-Allee 53, Freiburg, D-79110, Germany
[5] Research Unit Plant Genome and Systems Biology, Helmholtz Center Munich, D-85764 Neuherberg, Germany
[6] The James Hutton Institute, Invergowrie, Dundee, UK
[7] Facility for SYstems BIOlogy based MAss spectrometry, SYBIOMA, Proteomics Core Facility, KU Leuven, 3001 Leuven, Belgium
[8] Division of Crop Biotechnics, Laboratory of Tropical Crop Improvement, KU Leuven, 3001 Leuven, Belgium
[9] Research Unit Environmental Simulation, Helmholtz Center Munich, D-85764 Neuherberg, Germany
[10] Institut für Biologie und Biotechnologie der Pflanzen, Westfälische Wilhelms-Universität Münster, Schlossplatz 7, D-48149 Münster, Germany
[11] Faculty of Biological and Environmental Sciences, University of Helsinki, FIN-00014 Helsinki, Finland
[12] Department of Biochemistry, Max Planck Institute for Chemical Ecology, D-07745 Jena, Germany
[13] Research Group Plant Defense Physiology, Max Planck Institute for Chemical Ecology, D-07745 Jena, Germany
[†] Deceased 11 April 2023.
[‡] Deceased 16 May 2024.

* Correspondence: bastianleander.franzisky@hs-gm.de, baoguo.du@ctp.uni-freiburg.de, or maxim.messerer@helmholtz-munich.de

Received 8 June 2024; Editorial decision 31 October 2024; Accepted 7 November 2024

Editor: Kathy Steppe, Ghent University, Belgium

Abstract

Date palm (*Phoenix dactylifera* L.) is an important crop in arid regions and it is well adapted to desert ecosystems. To understand its remarkable ability to grow and yield in water-limited environments, we conducted experiments in which water was withheld for up to 4 weeks. In response to drought, root, rather than leaf, osmotic strength increased, with organic solutes such as sugars and amino acids contributing more to the osmolyte increase than minerals. Consistently, carbon and amino acid metabolism was acclimated toward biosynthesis at both the transcriptional and

Abbreviations: ABA, abscisic acid; CBP, Chl *a*/*b*-binding protein; GO, Gene Ontology; GSH, glutathione; JA, jasmonic acid; JA-Ile, jasmonoyl isoleucine; OA, osmotic adjustment; ROS, reactive oxygen species; SA, salicylic acid; TAG, triacylglycerol

translational levels. In leaves, a remodeling of membrane systems was observed, suggesting changes in thylakoid lipid composition which, together with the restructuring of the photosynthetic apparatus, indicated an acclimation preventing oxidative damage. Thus, xerophilic date palm avoids oxidative damage under drought by combined prevention and rapid detoxification of oxygen radicals. Although minerals were expected to serve as cheap key osmotics, date palm also relies on organic osmolytes for osmotic adjustment in the roots during early drought acclimation. The diversion of these resources away from growth is consistent with the date palm strategy of generally slow growth in harsh environments and clearly indicates a trade-off between growth and stress-related physiological responses.

Keywords: Antioxidant, halophyte, lipid metabolism, membrane remodeling, osmolyte, oxidative stress, *Phoenix dactylifera* L., reactive oxygen species, water deficit.

Introduction

Date palm (*Phoenix dactylifera* L.) is one of the most important crops in the semi- to hyperarid Arabian Peninsula. This is because it grows under a variety of extreme environmental conditions such as high soil salinity (Mueller *et al.*, 2023), heat, and water scarcity (Arab *et al.*, 2016; Du *et al.*, 2019, 2023; Kruse *et al.*, 2019). Climate change will lead to increased global temperatures and reduced regional precipitation and, thus, to an increased frequency of extreme events such as heat waves and summer drought (Amin *et al.*, 2016; Tabari and Willems, 2018; Saharwardi *et al.*, 2023). Understanding drought effects and development of drought-tolerant genotypes is central to deliver increased crop yield in environments of limited water availability (Chaves and Davies, 2010). However, plant responses to water deficit are complex (Puértolas *et al.*, 2017) and dependent on specific drought scenarios, differing in the extent of water scarcity, irrigation placement (Dodd *et al.*, 2008), and frequency (Boyle *et al.*, 2016).

In response to drought, many plants undergo rapid physiological changes due to osmotic stress, including an increase in abscisic acid (ABA) as a prominent feature that might indicate the water use strategy of a species or genotype (Sreenivasulu *et al.*, 2012). In addition to physiological functions in plant development, such as seed development, dormancy, and storage of proteins and lipids (Finkelstein *et al.*, 2002), ABA signaling mediates a rapid decrease of stomatal aperture to reduce transpirational water loss. In turn, this decreased stomatal conductance causes a drop in leaf internal carbon dioxide (CO_2) that negatively affects photosynthetic carbon fixation under water deficit (Cornic and Briantais, 1991; Brunner *et al.*, 2015). Date palm is a relatively slow-growing crop with sclerophyllous leaves that exhibit comparably low stomatal conductance even under well-watered conditions (Medrano *et al.*, 2002; Kruse *et al.*, 2019). This conservative water use strategy (Kruse *et al.*, 2019) is considered an evolutionary adaption to xeric environments (Mäkelä, 1996). In addition to stomatal regulation, ABA triggers the expression of several stress-responsive genes in numerous plant species, involved in the accumulation of protective proteins such as dehydrins and other late embryogenesis abundant proteins (Ingram and Bartels, 1996; Verslues *et al.*, 2006), and compatible osmolytes that contribute to lower the osmotic potential of the cell as part of osmotic adjustment (OA) (Chen and Murata, 2011; Slama *et al.*, 2015; Yaish, 2015). OA is an acclimation response to dehydration that helps to maintain turgor and protect specific cellular functions by stabilizing protein and membrane structures. It constitutes an important factor in plant survival and yield (Blum, 2017). Plants might accumulate as osmolytes both inorganic minerals such as potassium (K^+), chloride (Cl^-), and nitrate (NO_3^-) (Shabala and Shabala, 2011) as well as compatible organic compounds such as non-reducing sugars, polyols, and amino acids (Chen and Murata, 2011; Slama *et al.*, 2015). In comparison with OA by minerals, the accumulation of organic solutes takes place at an energetically higher cost (Yeo, 1983; Munns *et al.*, 2020). Still plants exposed to soil water deficit osmotically adjust to declining soil water potential predominantly using organic compounds (Munns *et al.*, 2020). Compared with the use of mineral solutes, this diverts significant amounts of photosynthetically fixed carbon and assimilated nitrogen from maintenance and growth processes. The type of organic osmolyte synthesized also impacts on related energy costs. The synthesis of sugars such as mannitol and sorbitol is cheaper in terms of water and nitrogen requirements than the synthesis of nitrogenous proline or glycine betaine. Recently, the cost in terms of carbon assimilated during the day has been calculated for OA in plants exposed to salt stress (Fricke, 2020; Munns *et al.*, 2020), which initially acts largely as hyperosmotic perturbation (Golldack *et al.*, 2011), and thus also requires OA. The diversion of 22– 66% of daily assimilated carbon for glucose-mediated OA in leaves and roots, respectively, highlights the high cost of using organic osmolytes for OA (Munns *et al.*, 2020).

The use of mineral osmolytes, although energetically more economical, is limited by the fact that high mineral ion concentrations, except for K^+, can interfere with metabolic reactions in all compartments of the cytoplasm (Shabala, 2013; Munns *et al.*, 2016). It is assumed that mineral ions are mainly used to adjust the osmotic pressure in the vacuole, while in the cytoplasm it is balanced by the accumulation of compatible organic osmolytes (Shabala, 2013). For example, the prominent

stress-induced accumulation of the compatible osmolyte proline makes a comparably small quantitative contribution to OA, but is associated with a protective effect on cellular functions and organs (Shabala and Shabala, 2011). Even under salt stress, when many minerals in the soil solution are available as cheap osmolytes, usually only half of the required additional osmolytes for OA are covered by mineral osmolytes (Munns *et al.*, 2020), generating an expensive demand for the synthesis of compatible organic solutes. Although energetically costly, the capability to osmotically adjust positively correlates with yield (Blum, 2017). Halophytes, such as date palm, are intrinsically characterized by tolerance to high tissue concentrations of mineral osmolytes such as K^+, Cl^-, and Na^+. Date palm is able to increase the intake of K^+ under high salinity (Mueller *et al.*, 2023), illustrating a remarkable capacity for adjusting its transportome to achieve selective K^+ intake in the face of hyperosmotic conditions and high external Na^+ concentrations. The preferential use of energetically favorable mineral osmolytes for OA is a trait considered to improve plant growth in future climatic conditions (Munns *et al.*, 2016; Munns and Millar, 2023). These adjustments also pose challenges for date palm productivity (Yaish and Kumar, 2015; Allbed *et al.*, 2017), despite date palm's remarkable ability to withstand extreme environmental conditions.

Date palms mitigate effects of heat and drought by employing proficient protein expression response comprising heat shock proteins and boosting of anti-oxidant activity to avoid oxidative stress (Safronov *et al.*, 2017). In addition, isoprene synthetase is up-regulated (Ghirardo *et al.*, 2021), which is thought to contribute to the protection of the photosynthetic apparatus from abiotic stress as part of the anti-oxidative machinery (Ryan *et al.*, 2014), as evidenced by increased isoprene emission (Arab *et al.*, 2016). Seasonal drought results in variable metabolic responses (Du *et al.*, 2021), including a shift in nitrogen metabolism that potentially facilitates a temporal accumulation of nitrogenous organic solutes, particularly in roots. However, there is limited information on drought-related OA of date palm, specifically regarding the use of energetically favorable mineral osmolytes versus more expensive organic solutes. To address this gap, a large-scale experiment that simulated the summer desert climate of the Arabian Peninsula was conducted, and osmotic and metabolic acclimation in date palm roots and leaves were analyzed.

It was hypothesized that (i) drought-exposed date palm preferentially relies on energetically favorable mineral osmolytes for OA, thus adapting the transportome in favor of mineral uptake, and (ii) its metabolism is acclimated by activating the anti-oxidative system to counteract increased reactive oxygen speciesm (ROS) formation. To address these hypotheses, we exposed date palm cv. Khalas to continuous drought and analyzed OA by relating mineral, sugar, and amino acid concentrations to changes in osmotic strength. To follow changes in mineral transporter expression and metabolic acclimation underlying organic solute synthesis and other drought acclimation responses, we performed transcriptome, proteome, and metabolite analyses in roots and leaves to elucidate how the xerophilic date palm thrives in arid deserts.

Materials and methods

Plant material and growth conditions

Seedlings of micro-propagated *Phoenix dactylifera* cv. Khalas of ~2 years old were purchased from Date Palm Developments Ltd (Somerset, UK). Seedlings were planted in 5 liter pots filled with 70% quartz gravel (3–5 mm diameter, Quarzwerke GmbH, Frechen, Germany) and covered by 4 cm of soil substrate (Floragard Vertriebs-GmbH, Oldenburg, Germany). For the drought experiment, plants were transferred into four, fully automated, climate-controlled walk-in phytotrons at the Research Unit of Environmental Simulation (EUS; Helmholtz Center Munich, Neuherberg, Germany). Conditions in phytotrons were slowly adjusted to match typical summer climate conditions for the period 21 June–21 September during 2003–2012 in Alahsa, Saudi Arabia (Kruse *et al.*, 2019), with average temperatures of ~40 °C at noon and 20 °C at night, and relative humidities of ~5% and 30%, respectively. The light period was set to 12 h, with a photon flux density of ~600 µmol photons m^{-2} s^{-1} at shoot height, which was lower than under natural conditions due to technical reasons. During the first 2 weeks in the phytotron, all plants were automatically irrigated with 50 ml of deionized water per plant every 4 h (i.e. 300 ml d^{-1}) so that all plants had comparable substrate water conditions and could acclimate to the climatic conditions. The use of deionized water was a mimic of natural low salinity irrigation. This well-watered irrigation regime corresponded to ~20% soil water content (SWC) measured at 5.5 cm substrate depth by using an ML2x ThetaProbe connected to an HH2 moisture meter (Delta-T, Cambridge, UK). After the initial 2 week acclimation period, drought treatment was initiated on a subset of plants by reducing irrigation to ~10% SWC, which was half the level of the well-watered regime. This water deficit has previously been shown to induce drought acclimation while ensuring plant viability (Kruse *et al.*, 2019; Ghirardo *et al.*, 2021). Specifically, the drought regime was initiated by withholding water for the first 3 d, resulting in progressive desiccation to ~10% SWC. Subsequently, the drought-regime plants received 50 ml of deionized water per plant daily, such that the SWC was maintained at a constant level of 10.7±5.2% for the remaining period of the experiment in the drought regime. Well-watered plants were continuously supplied with 50 ml of deionized water per plant every 4 h to maintain SWC at 21.4±7.5% throughout the experiment.

Ten individual plants per treatment and time point were entirely harvested between 12.00 h and 13.30 h, at 3, 10, and 31 d after the onset of the drought regime. Each plant was separated into shoot and roots for fresh weight analysis. These plant fractions were then immediately frozen in liquid nitrogen and stored at –80 °C until further processing at the end of the experiment, namely cutting and homogenization in liquid nitrogen and storage at –80 °C until further analysis.

Biomass and tissue hydration

The fresh weights of whole shoots and roots were measured at harvest. From each harvested individual plant fraction, specifically roots and shoot, a corresponding homogenized tissue sample was lyophilized. Tissue hydration was calculated by multiplying the difference between the hydrated weight and the weight after lyophilization by the reciprocal of the weight after lyophilization as previously described (Du *et al.*, 2021), to obtain the milliliters of water per gram of tissue dry mass. The individual hydration of the tissue fraction of each plant was the basis for calculating the osmolyte concentrations in the respective tissue water.

Fresh weight to dry weight conversion factors were assessed separately for each plant and its individual fractions, specifically roots and shoot. The initial hydrated mass was divided by the dry mass of the respective tissue to obtain the fresh to dry weight conversion factor. This factor was then multiplied by the corresponding fresh weights of the plant fractions recorded at harvest to calculate the dry weights of whole roots and shoots.

Transcriptome analysis

RNA library preparation and sequencing were done at the Biomedicum Functional Genomics Unit (FuGU, Helsinki, Finland). The total RNA input amounts used for ribo-depletion were 200 ng for leaf [Ribo-Zero rRNA Removal Kit (Plant Leaf), Illumina] and 1 µg for root samples [Ribo-Zero rRNA Removal Kit (Plant Seed/Root), Illumina]. Directional sequencing libraries were constructed using Illumina's ScriptSeq RNA Library Prep Kit. For this purpose, both mRNA and long non-coding RNA were sequenced from the samples. The resulting libraries were multiplexed and sequenced on an Illumina NovaSeq S1 flow cell 300 cycle flow cell (2×151 bp paired-end reads). The quality of the raw RNAseq reads was analyzed with FastQC (http://www.bioinformatics.babraham.ac.uk/projects/fastqc). The trimming step was performed with Trimmomatic (Bolger *et al.*, 2014) using the parameters 'ILLUMINACLIP:Illumina_PE_adapters.fasta:2:30:10:8:true LEADING:3 TRAILING:3 SLIDINGWINDOW:4:20 MINLEN:60'. The reads were mapped to a Trinity *de novo* assembly (Haas *et al.*, 2013) using Kallisto (Bray *et al.*, 2016). Assembly, construction, transcript annotation, and calculation of differentially expressed genes (DEGs) using EdgeR (Robinson *et al.*, 2010) were performed as described previously (Mueller *et al.*, 2023). DEG fold changes are given in base 2 logarithmic scale. Filtering for low read counts resulted in 70 285 transcripts. RNAseq data were submitted to EMBL-EBI-Annotare (https://www.ebi.ac.uk/fg/annotare) under the ArrayExpress accession number E-MTAB-14123.

Proteome analysis and computational integration in transcriptomic data

Protein extractions were performed following the phenol extraction/ammonium acetate precipitation protocol described previously (Carpentier *et al.*, 2005; Buts *et al.*, 2014). Briefly, after extraction, 20 µg of protein were digested with trypsin (Trypsin Protease, MS Grade ThermoScientific, Merelbeke, Belgium) and purified by Pierce C18 Spin Columns (ThermoScientific). The digested samples (0.5 µg 5 μl^{-1}) were separated in an Ultimate 3000 (ThermoScientific) UPLC system and then analyzed in an Orbitrap ELITE mass spectrometer (ThermoScientific) equipped with an Acclaim PepMap100 pre-column (Thermo Scientific) and a C18 PepMap RSLC (Thermo Scientific) using a linear gradient of buffer A and B (0.300 µl min^{-1}). Buffer A was composed of pure water containing 0.1% formic acid; buffer B was composed of pure water containing 0.08% formic acid and 80% acetonitrile. The Orbitrap ELITE mass spectrometer (ThermoScientific) was operated in positive ion mode with a nanospray voltage of 1.8 kV and a source temperature of 275 °C. The instrument was operated in data-dependent acquisition mode with a survey MS scan at a resolution of 60 000 for the mass range of m/z 375–1500 for precursor ions, followed by MS/MS scans of the top 20 most intense peaks with +2, +3, +4, and +5 charged ions. All data were acquired with Xcalibur 3.0.63.3 software (ThermoScientific). For protein quantification, the software Progenesis® (Nonlinear Dynamics) was applied using all peptides for quantification as described in Soares *et al.* (2018). We applied MASCOT version 2.2.06 (Matrix Science) against the assembled transcriptome using the search parameters parent mass tolerance of 12 ppm, fragment tolerance of 0.2 Da, variable modification by oxidation M, deamidation NQ, fixed modification by carbamidomethyl C, with up to two missed cleavages allowed for trypsin.

The transcriptomic data (51 494 features, Supplementary Table S1) were integrated with the proteomic data (4304 features, Supplementary Table S2). By searching the spectra against the mRNA database, transcript and protein abundances were linked to their genes (van Wesemael *et al.*, 2018). The genes identified in both omics analyses were filtered for drought-related changes at the protein level and then examined for over-representation in Gene Ontology (GO). Over-represented features related to plastid, anti-oxidant activity, and organic osmolyte metabolism were visualized using Cytoscape (Shannon *et al.*, 2003; Ma *et al.*, 2021).

Element analysis

The element concentrations of plant material were determined following acid digestion by inductively coupled plasma MS (ICP-MS) essentially as described previously (White *et al.*, 2012). Briefly, 50 mg dried samples were weighed and digested in closed vessels using a microwave digester (MARS Xpress; CEM Microwave Technology, Buckingham, UK). Samples were first digested with 3 ml of concentrated HNO_3 before the addition of 1 ml of 30% H_2O_2 to complete digestion. Digested samples were diluted to 50 ml with sterile MilliQ water before element analyses. Total K, Ca, Mg, P, S, Na, Cl, Fe, Mn, Zn, Cu, and Ni concentrations were determined on digested material by ICP-MS (Nexion 1000, PerkinElmer, Waltham, MA, USA). Blank digestions were performed to determine background concentrations of elements, and a tomato leaf standard (Reference 1573a; National Institute of Standards and Technology, NIST, Gaithersburg, MD, USA) was used as an analytical control.

Biochemical analyses

Analysis of anti-oxidants

Root and foliar H_2O_2 contents were determined according to Velikova *et al.* (2000) with modifications. H_2O_2 was extracted from ~50 mg of homogenized sample on ice with 1 ml of 0.1% (w/v) trichloroacetic acid (TCA). After centrifugation at 4 °C and 15 000 *g* for 15 min, an aliquot of 300 µl of the supernatant was added to 300 µl of 100 mmol potassium phosphate buffer (pH 7) and 600 µl of 1 mol KI. The absorbance was measured at 390 nm. H_2O_2 content was calculated using a standard curve ranging from 0 to 100 µM H_2O_2. *In vitro* glutathione reductase (GR) (EC 1.8.1.7) and glutathione dehydroascorbate reductase (DHAR) (EC 1.8.5.1) activities in leaves were determined as described previously (Arab *et al.*, 2016). Briefly, GR activity was quantified by monitoring glutathione (GSH)-dependent oxidation of 1.25 mM NADPH at 340 nm; DHAR activity was analyzed by following the increase in absorbance at 265 nm, resulting from GSH-dependent production of ascorbate (Polle *et al.*, 1990). Thiols (i.e. total and oxidized GSH, cysteine, and γ-glutamylcysteine) were extracted as described in Schupp and Rennenberg (1988) from ~40 mg of homogenized sample with 1 ml of 0.1 M HCl containing 100 mg of pre-washed polyvinylpolypyrrolidone. Quantification of oxidized glutathione (GSSG) was based on the irreversible alkylation of the free thiol groups of the GSH with *N*-ethylmaleimide (NEM), and the subsequent reduction of GSSG with DTT (Strohm *et al.*, 1995). Thiol derivatives were separated on an ACQUITY UPLC®HSS (Waters, Eschborn, Germany) with a C-18 column (2.1×50 mm; 1.18 µm mesh size) applying a solution of potassium acetate (100 mM) in methanol (100%) for elution. Concentrations of thiols were quantified according to a mixed standard solution consisting of GSH, cysteine, and γ-glutamylcysteine subjected to the same reduction and derivatization procedure. Reduced thiols were quantified as monobromobimane derivatives after separation by UPLC by fluorometric analysis (Samuilov *et al.*, 2016). Total and reduced ascorbate were determined using a colorimetric method previously described in Arab *et al.* (2016). Briefly, ~50 mg of homogenized sample was extracted in 500 µl of 5% meta-H_3PO_4, mixed, and centrifuged at 4 °C for 30 min at 12 000 *g*. A 100 µl aliquot of the supernatant was mixed with 20 µl of

1.5 M triethanolamine and 100 µl of 150 mM sodium phosphate buffer (pH 7.4) in separate safe-seal 2 ml tubes for reduced and total ascorbate quantification. Total ascorbate was measured post-reduction by adding 50 µl of 10 mM DTT and incubating at room temperature for 15 min, followed by removal of excess DTT with 50 µl of 0.5% NEM. Further preparation for ascorbate determination involved adding 200 µl each of 10% TCA, 44% orthophosphoric acid, 4% 2,2′-dipyridil in ethanol, and 100 µl of 3% (w/v) $FeCl_3$. The solutions were mixed and incubated at 37 °C for 60 min. Absorbance was measured at 525 nm using a spectrophotometer.

Analysis of water-soluble metabolites

Relative abundances of water-soluble low molecular weight metabolites in leaves were analyzed by GC-MS as described previously (Du *et al.*, 2019). Briefly, ~50 mg of homogenized sample was transferred into pre-frozen 2 ml tubes, 600 µl of cold 100% methanol was used as the extraction solvent, and 60 µl of ribitol (0.2 mg ml^{-1} in ddH_2O) was added as an internal standard. Samples were heated to 70 °C and shaken at 1200 *g* for 10 min. After centrifugation, 500 µl aliquots of the supernatant were mixed with an equal volume of double-distilled H_2O and chloroform. The mixtures were vigorously shaken and centrifuged at 14 000 *g* at 4 °C for 5 min. Aliquots of 100 µl of the methanol phase were transferred to 1.5 ml tubes and dried using a freeze dryer. Dried methanol extracts were methoximated by adding 20 µl of a 20 mg ml^{-1} methoxyamine hydrochloride solution in anhydrous pyridine. The samples were incubated at 30 °C for 90 min while shaking at 1400 *g*. For trimethylsilylation, 35 µl of *N*-methyl-*N*-(trimethylsilyl) trifluoroacetamide was added, and the mixtures were incubated at 37 °C for 30 min with shaking at 1400 *g*. A 5 µl aliquot of *n*-alkane retention index calibration standard (*n*-alkane mix, C10–C40, 50 µg ml^{-1} in *n*-hexane) was then added. Following brief mixing, the mixtures were centrifuged at 14 000 *g* and 20 °C for 2 min. Finally, 50 µl of the supernatant was transferred to vials for GC-MS analysis essentially as described elsewhere (Kreuzwieser *et al.*, 2009). Peak identification and chromatogram deconvolution were conducted with the Quantitative Analysis Module of MassHunter software (Agilent Technologies, Böblingen, Gemany). Metabolite identification was performed using the Golm metabolome database (Hummel *et al.*, 2010), with metabolite abundances derived from normalized peak areas.

Analysis of phytohormones

Phytohormone extraction and subsequent LC-MS analysis were performed as described elsewhere (Vadassery *et al.*, 2012; Dávila-Lara *et al.*, 2021). Briefly, ~50 mg of homogenized sample was extracted with 1.5 ml of methanol containing 60 ng of D6-ABA (Toronto Research Chemicals, North York, ON, Canada), 60 ng of D6-jasmonic acid (JA; HPC Standards GmbH, Borsdorf, Germany), 60 ng of D4-salicylic acid (SA; Santa Cruz Biotechnology, Dallas, TX, USA), and 12 ng of D6-jasmonoyl-isoleucine conjugate (JA-Ile; HPC Standards GmbH) as internal standard. Phytohormone analyses were carried out by LC-MS/MS on an Agilent 1260 series HPLC system (Agilent Technologies) with a tandem mass spectrometer QTRAP 6500 (SCIEX, Framingham, MA, USA). Chromatographic separation and MS were performed according to Dávila-Lara *et al.* (2021).

Analysis of amino acids

Amino acid concentrations were analyzed with modifications as described by Döring *et al.* (2022). Briefly, 30 mg of freeze-dried powder was dissolved in 1 ml of buffer (0.12 M Li-citrate, 100 nM norleucine, pH 2.2). For extraction, samples were placed in an ultrasonic bath (Super RK 1028, Bandolin, Germany) cooled to 20 °C and constantly sonicated for 15 min. After centrifugation for 15 min at 15 000 *g*, the supernatant was filtered through a 0.45 µm nylon filter and transferred to vials for measurement. Chromatography of unbound amino acids was performed over 2 h on an amino acid analyzer S433 using a 4.6×150 mm LCA K 07/Li cation-exchange column (Sykam, Eresing, Germany). Automatic post-column ninhydrin derivatization was applied before primary and secondary amino acids were detected photometrically at 570 nm and 440 nm, respectively.

Analysis of soluble sugar and starch

Soluble sugar and starch concentrations were determined using the modified anthrone colorimetric method as described elsewhere (Li *et al.*, 2013). Briefly, 50 mg of dried and ground sample were mixed with 5 ml of 80% ethanol and heated to 80 °C for 30 min. After centrifugation at 5000 *g* for 5 min, the supernatant was collected. This extraction was repeated and supernatants were combined for soluble sugar analysis, while the precipitates were used for starch determination. To analyze starch, 2 ml of distilled water were added to the precipitates and heated in boiling water for 15 min. After cooling, 2 ml of 9.2 M $HClO_4$ were added to hydrolyze the starch for 15 min. Then, 4 ml of distilled water were added and supernatant was collected after centrifugation at 5000 *g* for 10 min. Starch hydrolyzation was repeated and supernatants were combined for analysis. Both extracts were analyzed spectrophotometrically at 620 nm using glucose as a standard. Starch levels were calculated by multiplying glucose concentration by the conversion factor of 0.9 (Osaki *et al.*, 1991).

Osmolarity analysis

Osmolarity was measured using a semi-micro osmometer (Knauer ML, Berlin, Germany). To prepare the sample, 150 µl of the soluble sugar extract as described above was dried at 45 °C to evaporate the ethanol. Next, 150 µl of distilled water was added, and the solution was mixed vigorously before measuring according to the manufacturer's protocol.

Statistical analysis

Data presented are from a large-scale experiment comparing different environmental factors with one control group; the control data are similar to those presented elsewhere (Du *et al.*, 2023; Mueller *et al.*, 2023). The experiment included a well-watered 'control' and a water deficit 'drought' condition. Ten replicates (whole date palms) from each condition were sampled at 3, 10, and 31 d following the onset of the water deficit regime. Data processing, ANOVA, models, and post-hoc tests (Tukey's) were performed using R (R Core Team, 2013). To analyze the effects of drought exposure and its duration, the watering regime, exposure period, and their interaction were entered as independent variables into linear models. Homogenity of data distribution was checked using the Shapiro–Wilk algorithm of 'stats'. Inhomogeneously distributed data were logarithmically transformed and the normal distribution of the model residuals was verified or, if inadequate, the data were tested using the Kruskal–Wallis algorithm. Analyses were performed with various numbers of replicates: biomass and tissue hydration, n=5; ionome, n=5–10; phytohormones, n=5–10; metabolome, anti-oxidants, soluble sugars, and osmolarity, n=5; proteome, n=4; RNA-sequencing, n=3. Datasets with unbalanced sample sizes were evaluated using the HSD. test algorithm of 'agricolae' (de Mendiburu, 2019) with the argument for unbalanced enabled. A significance threshold of $P \leq 0.05$. was applied. For osmolyte correlation analysis, a missing tissue hydration value (root_control_day1) was median imputed from remaining replicates. The relative importance of dependent variables in linear regressions was calculated using 'relaimpo' (Grömping, 2007). Data were plotted using 'ggplot2' (Wickham, 2016) and 'pheatmap' (Kolde, 2015).

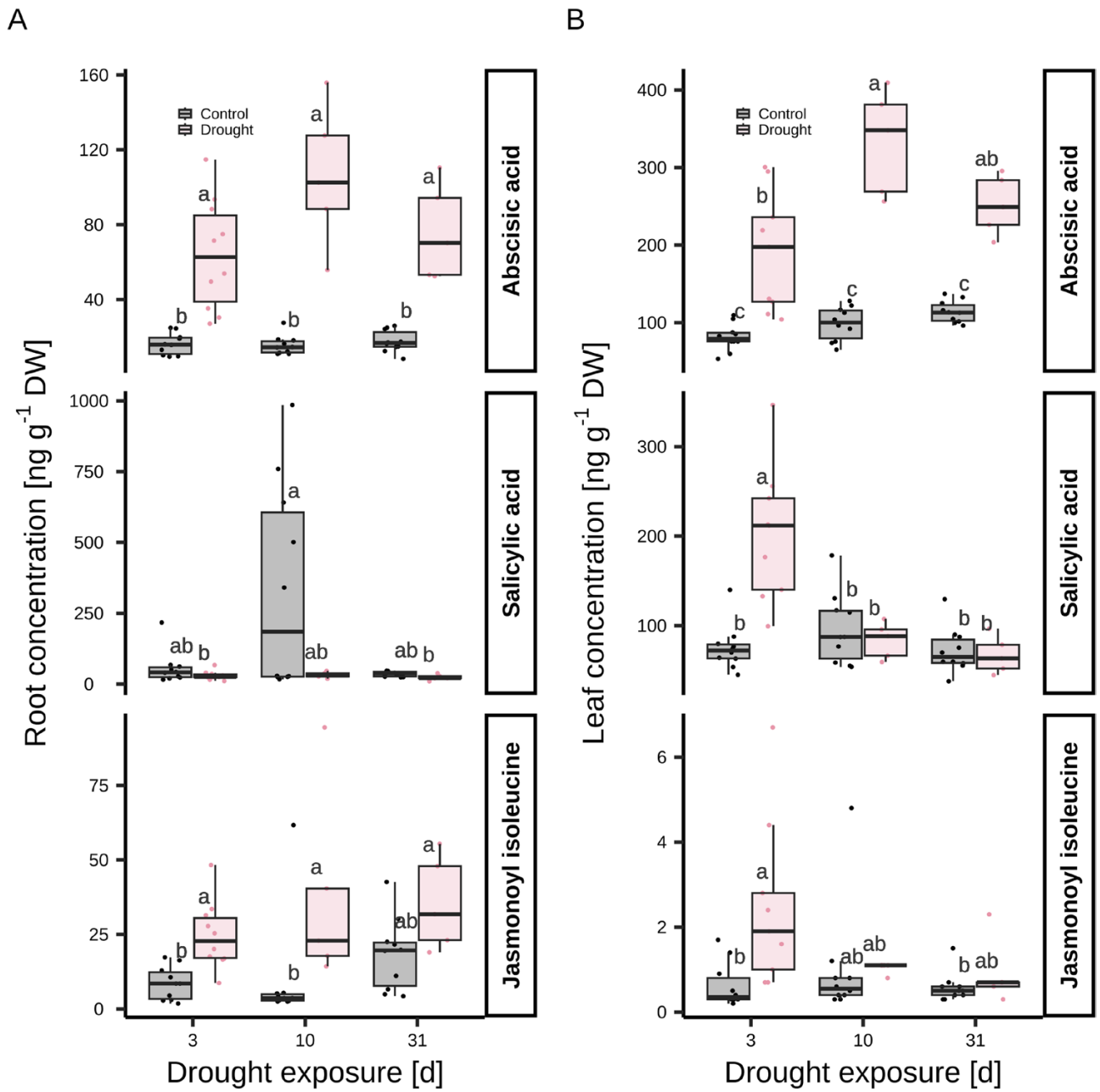

Fig. 1. *Phoenix dactylifera* cv. Khalas accumulates abscisic acid in roots and leaves and jasmonoyl-isoleucine mainly in roots under drought. Concentrations of abscisic acid, salicylic acid, and jasmonoyl-isoleucine in (A) roots and (B) leaves of date palms grown in phytotrons simulating Saudi Arabia summer climate conditions after 3, 10, and 31 d under well-watered or drought regimes. Data are presented as box plots featuring the maxima, 75 quartiles, medians, 25 quartiles, and minima. Points shown represent raw data; n=10–5; Tukey's, $P \leq 0.05$; different letters indicate significant differences of comparisons between water regime and time point.

Results

Drought leads to accumulation of abscisic acid and activation of anti-oxidative metabolism in both roots and leaves

After 3 d of drought exposure, ABA concentrations in roots were increased to 60 ng g^{-1} DW, reaching a peak of 105 ng g^{-1} DW after 10 d of drought, while well-watered controls remained at ~16 ng g^{-1} DW throughout the experiment (Fig. 1A). A similar ABA pattern was observed in leaves (Fig. 1B), but at higher concentrations than in roots. Well-watered controls showed concentrations ranging from 90 ng to 110 ng ABA g^{-1} DW. Under drought, ABA increased to 190 ng g^{-1} DW after 3 d, reaching a maximum of 330 ng g^{-1} DW after 10 d and 250 ng g^{-1} DW after 31 d. Similar to ABA, the bioactive derivate of JA, JA-Ile, accumulated in roots under drought

(Fig. 1A). After 3–31 d of drought, JA-Ile was increased to ~25 ng g^{-1} DW compared with the control of ~10 ng g^{-1} DW. In leaves, higher JA-Ile concentrations were only observed after 3 d of drought, but at generally lower concentrations with a maximum at ~2 ng g^{-1} DW (Fig. 1B).

Concurrent with the peak in ABA concentration after 10 d of drought exposure (Fig. 2), leaves showed an increase in H_2O_2 content that was still present after 31 d. With the increase in this ROS, metabolites and enzymes involved in ROS detoxification were up-regulated, as evidenced by, for example, increased foliar levels of ascorbic acid, GSH, and glutathione disulfide at 10 d and 31 d of drought exposure and increased GR activity after 10 d. In roots, H_2O_2 did not accumulate with short or long drought exposure. Accordingly, the response of the anti-oxidative system was less pronounced in the roots than in the leaves. However, there were drought-related increases in the levels of dehydroascorbic acid, GSH, and glutathione disulfide. Also, the activities of DHAR and GR were increased after 3 d of drought exposure, and the GR activity also after 10 d.

The increased anti-oxidative demand as a result of drought exposure was also evident at the protein level after 31 d of drought exposure. In roots, 10 proteins were annotated to the molecular function 'antioxidant activity' (GO:0016209) (Fig. 3A), with ascorbate peroxidases 1, 2, and 3, NADPH-dependent thioredoxin reductase 2, and glutathione *S*-transferases PHI9 consistently increased in response to 31 d of drought. In leaves, catalase 2 was annotated to 'oxidoreductase activity' (GO:0016491), with two of the five detected homologs showing ~0.7-$fold_{log2}$ decreased protein levels (Fig. 3B), while two homologous copper/zinc superoxide dismutases 2, annotated to the cellular component 'plastid', were about doubled after 31 d of drought.

Proteomic and transcriptomic insights reveal drought-induced protein stabilization and membrane remodeling in date palm leaves

Proteomic analysis revealed that in response to 31 d of drought exposure, the leaves showed a remarkable accumulation of numerous protein-stabilizing chaperones that were annotated to 'protein folding' (GO:0006457). Heat shock-like protein and HSP20-like chaperone superfamily protein were doubled in abundance. Chaperonin 20, Chaperonin 60 alpha, and heat shock cognate protein 70 were associated with the cellular compartment 'plastid' (GO:0009536; Fig. 3) and showed increased protein levels ranging from 0.5- to 1-$fold_{log2}$. This suggests a need for protein stabilization in plastids after drought exposure. Consistently, among the 23 proteins annotated to 'plastid', PSII subunit O-2, and PSII oxygen-evolving complex 1 showed decreased abundance, while the abundance of chlorophyll A-B-binding family protein, involved, for example, in modification of antenna complexes (Zolla and Rinalducci, 2002), was nearly doubled.

Transcript analysis revealed that with respect to plastid-associated lipid metabolism, drought-induced changes were evident (Supplementary Table S1C), suggesting a drought-related remodeling of the lipid composition to stabilize membrane systems and embedded proteins. In this context, a 2-$fold_{log2}$ increase in transcripts of two digalactosyldiacylglycerol synthase homologs and a 2-$fold_{log2}$ up- and 6-$fold_{log2}$ down-regulation of two homologous monogalactosyldiacylglycerol synthases suggested an alteration in the biosynthesis of galactosylated diacylglycerols in favor of an increase in the ratio of poly- to mono-galactosylated diacylglycerols, which improves thylakoid stability during dehydration (Chng *et al.*, 2022). Consistently, transcripts of a set of eight genes encoding

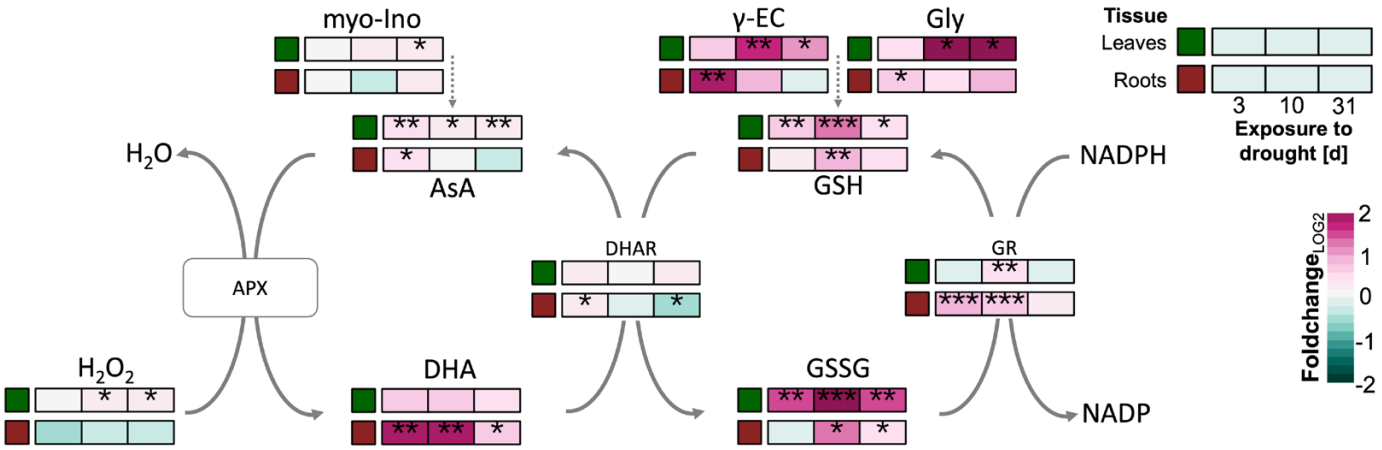

Fig. 2. Anti-oxidative activity is stimulated in both roots and leaves of *Phoenix dactylifera* cv. Khalas under drought, yet foliar oxygen radicals accumulate. Response of metabolites and enzymes assigned to the Foyer–Halliwell–Asada cycle in leaves and roots of date palms grown in phytotrons simulating Saudi Arabia summer climate conditions after 3, 10, and 31 d under well-watered or drought regimes. APX, ascorbate peroxidase activity; AsA, reduced ascorbate; DHA, dehydroascorbate; DHAR, dehydroascorbic acid reductase activity; Gly, glycine; GR, glutathione reductase activity; GSH, total glutathione; GSSG, glutathione disulfide; myo-Ino, myo-inositol; γ-EC, gamma-glutamylcysteine. Means of the fold-change$_{log2}$ are indicated by a color code (n=5; t-test; *P≤0.05; **P≤0.01; ***P≤0.001).

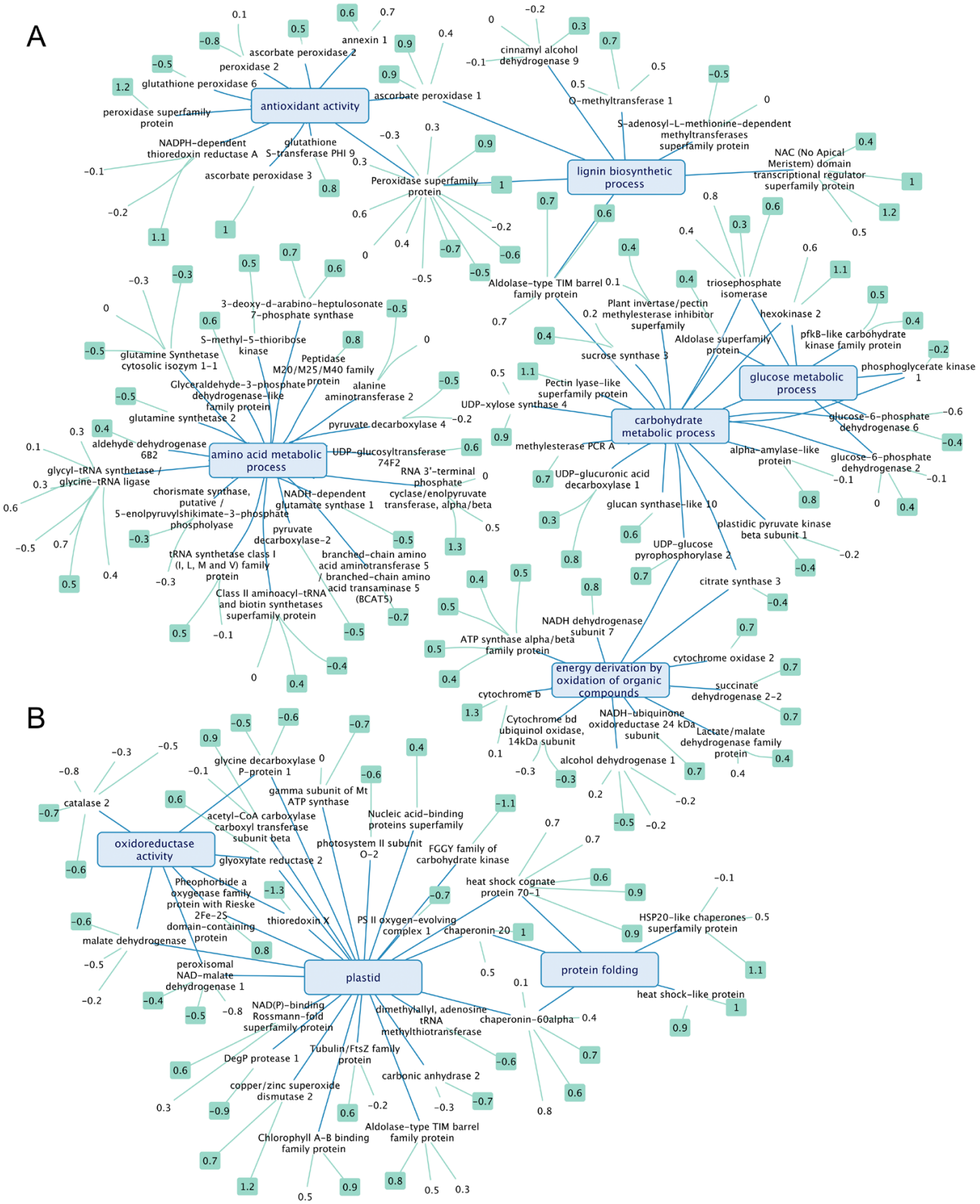

Fig. 3. Changes in protein levels in roots and leaves of *Phoenix dactylifera* cv. Khalas in response to a 4 week drought exposure. Networks based on combined transcriptomic and proteomic data reveal strong responses of (A) roots and (B) leaves to 31 d of drought exposure. Transcriptome data were

integrated with proteome data to match detected protein and underlying mRNA. Over-represented Gene Ontology (GO) terms were identified based on drought-responsive proteins. GO terms with respect to the three domains 'Molecular function', 'Biological process', and 'Cellular component' are shown in blue network hubs. Node labels on blue edges show individual gene annotations. Each of the rectangular-shaped boxes in the outer layer represents a protein feature annotated to the respective gene. Turquoise coloring of the outermost node indicates a significant change at the protein level (n=4; $P \leq 0.05$), which could be either an increase or a decrease as indicated by a fold-change$_{log2}$.

subunits of the lipid importer complex (TGD2,3,4), involved in trigalactosyldiacylglycerol import into the plastid (Fan *et al.*, 2015), were also increased.

With respect to glycosylation of sterols, which are important for the regulation of the physical properties of membranes (i.e. the permeability of membranes to hydrophilic molecules), a trend towards a reduced glycosylation was suggested, as the transcripts of three homologs of UDP-glycose:sterol glucosyltransferase were consistently reduced. Changes in sterol glycosylation might affect the organization of lipids and proteins within the membrane (Singh *et al.*, 2018).

Drought-related changes in the metabolism of sphingolipids, which are integral structural components of the plasma membrane that affect its permeability and fluidity, and are involved in the formation of microdomains called lipid rafts that facilitate protein trafficking (Sharma *et al.*, 2023), are also likely. Three genes involved in sphingolipid metabolism—ceramide kinase, catalytic subunit 1 of serine C-palmitoyltransferase complex, and inositol phosphosphorylceramide synthase—exhibited 2-fold$_{log2}$ decreased transcript levels. Conversely, transcripts of ceramide glycosyltransferase, a key enzyme in sphingolipid metabolism that generates the precursor for all glycosphingolipids—glucosylceramide—were ~4-fold$_{log2}$ increased. Along with these changes, two homologous glycosylinositol phosphorylceramide mannosyltransferases, a Golgi-localized glycosylinositol phosphorylceramide-specific mannosyl-transferase (Ali *et al.*, 2018), and a sphingolipid fatty acid 2-hydroxylase that catalyzes the 2-hydroxylation of the sphingolipid *N*-acyl chain (Hama, 2010) were up-regulated >2-fold$_{log2}$, revealing that the overall expression of genes involved in the biosynthesis of sphingolipids was up-regulated in response to drought. With respect to triacylglycerol (TAG) synthesis, transcripts of three homologs of acyl-CoA:diacylglycerol acyltransferase (DGAT1,2) were 2-fold$_{log2}$ up-regulated by drought exposure. DGAT plays a key role in determining the flux of carbon into TAGs by catalyzing the only step exclusively dedicated to TAG synthesis (Liu *et al.*, 2012; Jin *et al.*, 2017), thus favoring TAG accumulation (Hatanaka *et al.*, 2022) in date palm leaves after 31 d of drought exposure.

Drought inhibits plant growth and causes accumulation of osmolytes

Given that date palm is a slow-growing species and the 31 d experimental period is short relative to a full growing season, no significant difference in root biomass was observed between well-watered and drought-exposed plants, with both maintaining an average of ~7 g DW per plant throughout the experiment (Fig. 4A). In contrast, a significant reduction in shoot mass was observed as a result of drought exposure, which was evident after 10 d and amounted to ~50% after 31 d compared with the shoot of the well-watered control (Fig. 4B). The hydration of the root remained unaffected independent of drought exposure at ~3.25 g H_2O g^{-1} DW (Fig. 4C). The leaves showed a lower hydration compared with the roots, with values of ~1.8 g H_2O g^{-1} DW, which also remained unchanged despite the drought (Fig. 4D). In a first attempt to monitor the change in osmotic strength as a result of acclimation to drought exposure, total osmolytes were extracted and related to tissue water content. In the leaves, osmolyte concentrations were ~300 mM irrespective of the duration of drought exposure (Fig. 4F). Root osmolyte concentrations were lower and remained at ~125 mM under well-watered conditions (Fig. 4E). In response to drought exposure, the concentration increased over the course of drought exposure, resulting in a final concentration of ~275 mM after 31 d, representing a significant increase of 130% compared with the control. To determine the types and individual contributions of osmolytes responsible for this significant increase in osmotic strength of date palm roots, we analyzed the concentrations of ions, soluble sugars, and amino acids.

Mineral osmolytes do not play a major role following drought exposure

Regarding halophytes, K^+, Cl^-, and Na^+ are considered the major mineral osmolytes involved in cellular OA (Shabala and Shabala, 2011). The total concentration of these ions in roots was ~0.7 mmol g^{-1} DW without any significant changes in response to the drought exposure (Fig. 5A). However, analysis of individual mineral concentrations in roots revealed that K^+ concentrations increased by ~30% in roots after 31 d of drought compared with the well-watered control (Fig. 5C), while changes in Cl^- and Na^+ concentrations were not significant (Fig. 5E). In leaves, the total mineral osmolyte concentration was ~0.8 mmol g^{-1} DW (Fig. 5B) and was also not significantly affected by drought exposure. In both roots and leaves, the concentrations of other minerals such as Ca, Mg, P, S, Cu, Fe, Mn, Ni, Na, and Zn showed no significant or marginal changes in response to drought exposure (Supplementary Fig. S1).

To identify changes in mineral transporter expression associated with the increase in root K^+ concentrations in response to drought, we analyzed the transcriptome of roots and leaves

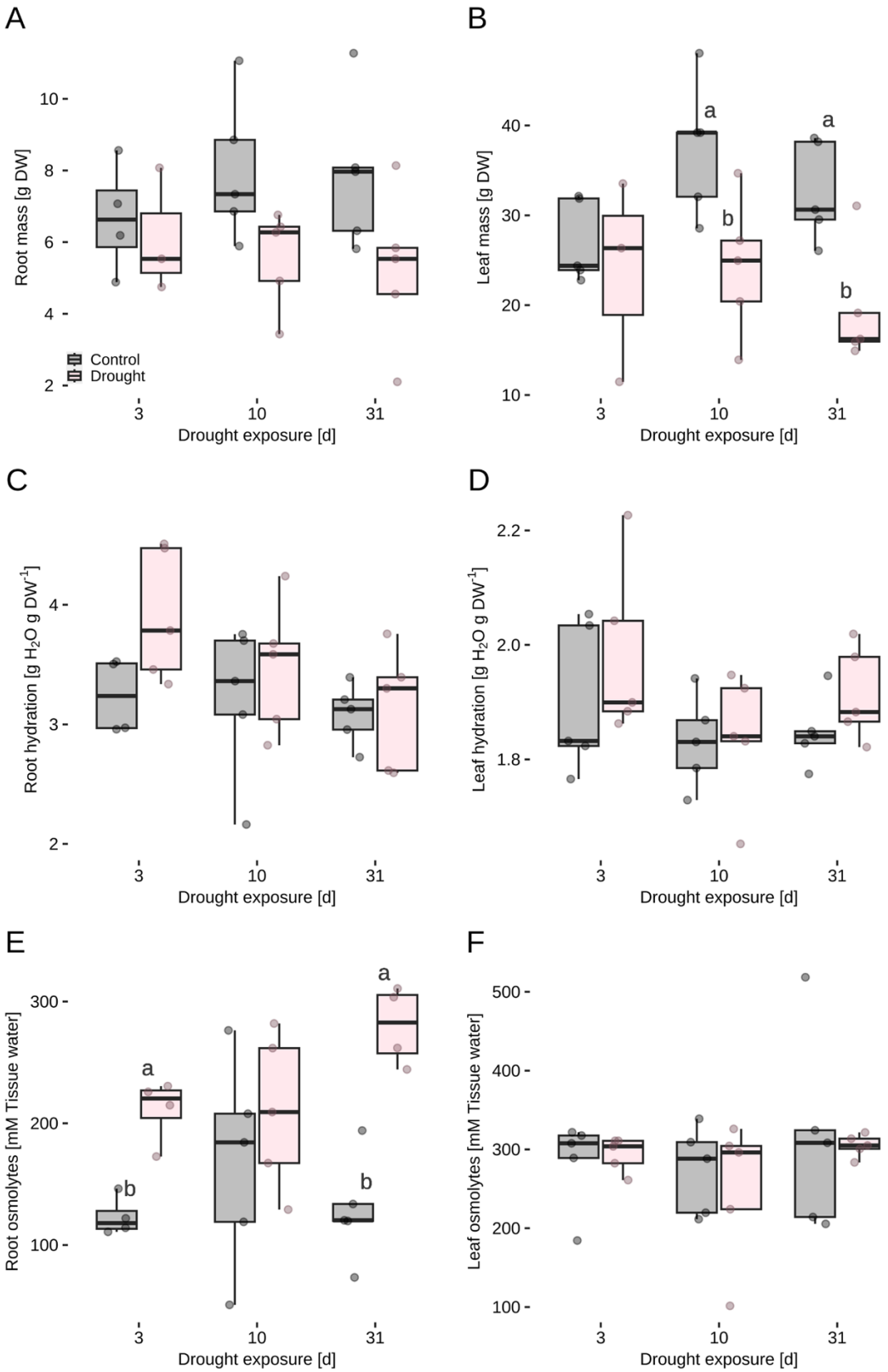

Fig. 4. Root and leaf growth of *Phoenix dactylifera* cv. Khalas stagnates under drought stress, while tissue hydration remains unaffected with a parallel increase in osmolyte concentration. Biomass of (A) roots and (B) leaves, tissue hydration of (C) roots and (D) leaves, and osmolyte concentration of (E) roots and (F) leaves of date palms grown in phytotrons simulating Saudi Arabia summer climate conditions after 3, 10, and 31 d under well-watered (control) or drought conditions. Data are presented as box plots featuring the maxima, 75 quartiles, medians, 25 quartiles, and minima. Points shown represent raw data; $n_{Biomass}$=5, $n_{Hydration}$=5; $n_{Osmolytes}$=5–4; Tukey's, $P \leq 0.05$; different letters indicate significant differences of water regime comparison within a time point; no letters, $P > 0.05$. Color code as shown in (A) for all panels.

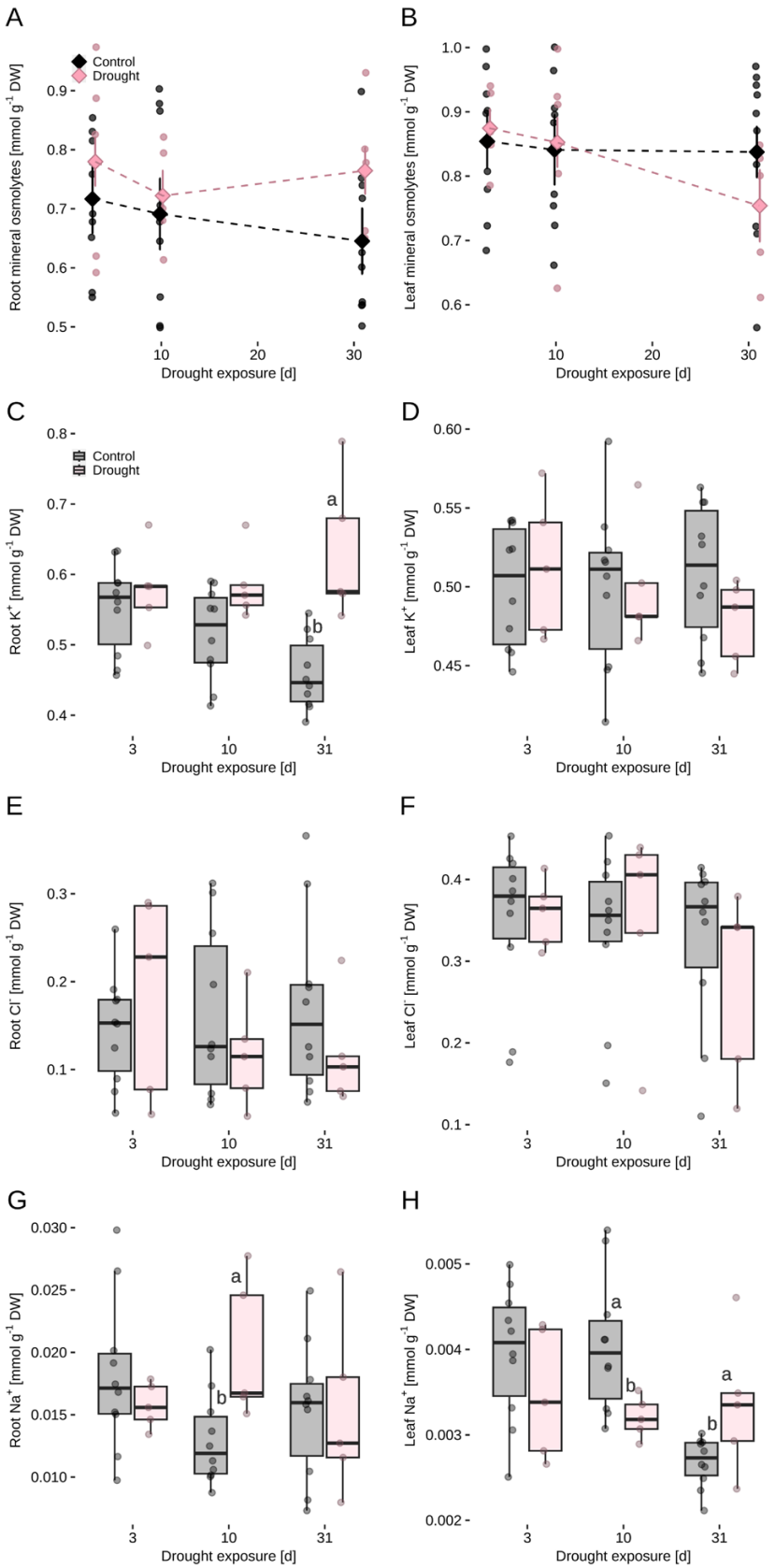

Fig. 5. Mineral osmolyte concentration in roots of *Phoenix dactylifera* cv. Khalas remains unaffected during 4 weeks of drought exposure. Total concentration of the major mineral osmolytes of halophytes [potassium (K^+), chloride (Cl^-), and sodium (Na^+)] in (A) root and (B) leaf, and individual mineral concentrations in roots and leaves, respectively, of K^+ (C) and (D), of Cl^- (E) and (F), and of Na^+ (G) and (H) of date palms grown in phytotrons simulating Saudi Arabia summer

climate conditions after 3, 10, and 31 d under well-watered (control) or drought conditions. (A, B) Means ±SE; (C–H) Data are presented as box plots featuring the maxima, 75 quartiles, medians, 25 quartiles, and minima. Points shown represent raw data; n=10–5; Tukey's, $P \leq 0.05$; different letters indicate significant differences of water regime comparison within a time point; no letters, $P > 0.05$. Color code as shown in (A) or (C) for all panels.

after 31 d of drought exposure. Despite the drought-related increase in K^+ concentration in date palm root, only a few K^+ transporter genes were differentially expressed after 31 d of drought. Among a total of 187 K^+ transport-related genes identified, only AKT2/3, a bidirectional channel, was found to be significantly up-regulated in the roots, but to a strong extent of ~40-fold$_{log2}$ (Supplementary Table S1A, B). Consistent with the K^+ concentrations in the leaves not being affected by drought, 12 K^+ transport-related genes were differentially regulated, with seven up-regulated (up to 14-fold$_{log2}$) and five down-regulated (up to 3-fold$_{log2}$).

Drought-related sugar accumulation in roots is favored by up-regulation of oligosaccharide biosynthesis

Accumulation of oligosaccharides contributes to root osmotic adjustment

Measurement of total soluble sugar concentration in roots revealed a marked increase in response to 31 d of drought exposure (Fig. 6A), while no effect of drought was observed in leaf sugars. From 3 d to 10 d of drought, root sugar concentrations of ~0.4 mmol g^{-1} DW were not significantly higher than those of the control. However, individual sugars indicated early changes in composition already after 3 d of drought, with up to 0.8-fold$_{log2}$ increases in galactinol and myo-inositol (Fig. 6E), while after 10 d of drought, arabinose, gentiobiose, and trehalose were increased by 0.6- to 3-fold$_{log2}$. After 31 d of drought, there was a significant increase in total sugars to ~0.5 mmol g^{-1} DW (Fig. 6A), an increase of ~80% compared with well-watered controls. Concurrent with this marked increase, a diverse range of sugar compounds was increased (Fig. 6E), with 2-fold$_{log2}$ increases in fructofuranosyl-fructofuranose and gentobiose, and 1-fold$_{log2}$ increases in idose, myo-inositol, and mannose, while the disaccharide sophorose was decreased. Although the leaves did not show an increase in total soluble sugars in response to drought exposure (Fig. 6B), the sugar composition was significantly altered (Fig. 6E), with 1- to 3-fold$_{log2}$ increases in galactinol and raffinose, while arabinose was decreased, beginning 3 d after drought exposure. Other sugars, such as fructose, 6-deoxy-mannopyranose, and glucose derivatives, also increased up to 1-fold$_{log2}$, but not consistently.

Acclimation of root carbohydrate metabolism to drought favors oligosaccharide biosynthesis

Consistent with the marked increase in soluble sugar concentrations in roots (Fig. 6A), carbohydrate metabolism was significantly altered after 31 d of drought. Transcripts of genes related to oligosaccharide metabolism showed a coherent increase of four galactinol synthases (3- to 7-fold$_{log2}$) and one stachyose synthase (10-fold$_{log2}$) (Supplementary Table S1F) that both favor the synthesis of oligosaccharides (Li *et al.*, 2020). Consistently, analysis of proteomic responses revealed enrichment of 20 proteins that were annotated to the biological processes 'carbohydrate metabolic process' (GO:0005975) and 'glucose metabolic process' (GO:0006006) (Fig. 3A). Protein levels of glucose-6-phosphate dehydrogenase 2 and 6 homologs were ambiguously changed in response to drought, while other proteins of root carbohydrate metabolism, such as phosphoglycerate kinase 1 and citrate synthase 3, were significantly increased, suggesting increased abundance of enzymes involved in oligosaccharide biosynthesis. In leaves, the transcript levels of genes related to carbohydrate metabolism and raffinose-family oligosaccharides such as galactinol synthases were ambiguously changed, with one homolog 9-fold$_{log2}$ decreased while two others were ~3- and 14-fold$_{log2}$ increased (Supplementary Table S1F), reflecting the increase in raffinose in leaves under drought (Fig. 6E). Genes related to starch metabolism were also differentially expressed, suggesting a trend toward decreased starch synthesis and increased starch degradation, which might favor the conversion of carbon moieties from starch into oligosaccharides with greater contribution to OA. Transcripts of four genes involved in starch formation were coherently decreased, including two starch synthases with 8- and 2-fold$_{log2}$ reduction. Some genes involved in starch degradation also had lower transcripts, such as phosphoglucan phosphatase and starch-debranching pullulanase. However, transcripts of two homologs of each of the alpha- and beta-amylases involved in starch degradation were increased by 2- to 5-fold$_{log2}$, revealing an acclimation towards starch degradation in favor of oligosaccharides, although total starch content of the leaf remained unchanged (Fig. 6D).

Amino acid accumulation under drought is supported by enhanced biosynthesis

Amino acids accumulate during long-term drought exposure

In both control and drought-stressed date palm roots, the total amino acid concentration was ~190 µmol g^{-1} DW after 3 d and 10 d of exposure to drought (Fig. 7A). However, after 31 d of drought, the amino acid concentration was significantly higher by ~110 µmol g^{-1} DW, which was double that of the control. In leaves of the well-watered control, the concentration of amino acids remained constant at ~20 µmol g^{-1} DW throughout the experiment (Fig. 7B). Under drought conditions, the concentration increased to a maximum of 45 µmol g^{-1} DW after 10 d, and then returned to a level similar to the control at ~30 µmol g^{-1} DW after 31 d. Subsequently, the contribution of individual amino acids to these changes was evaluated.

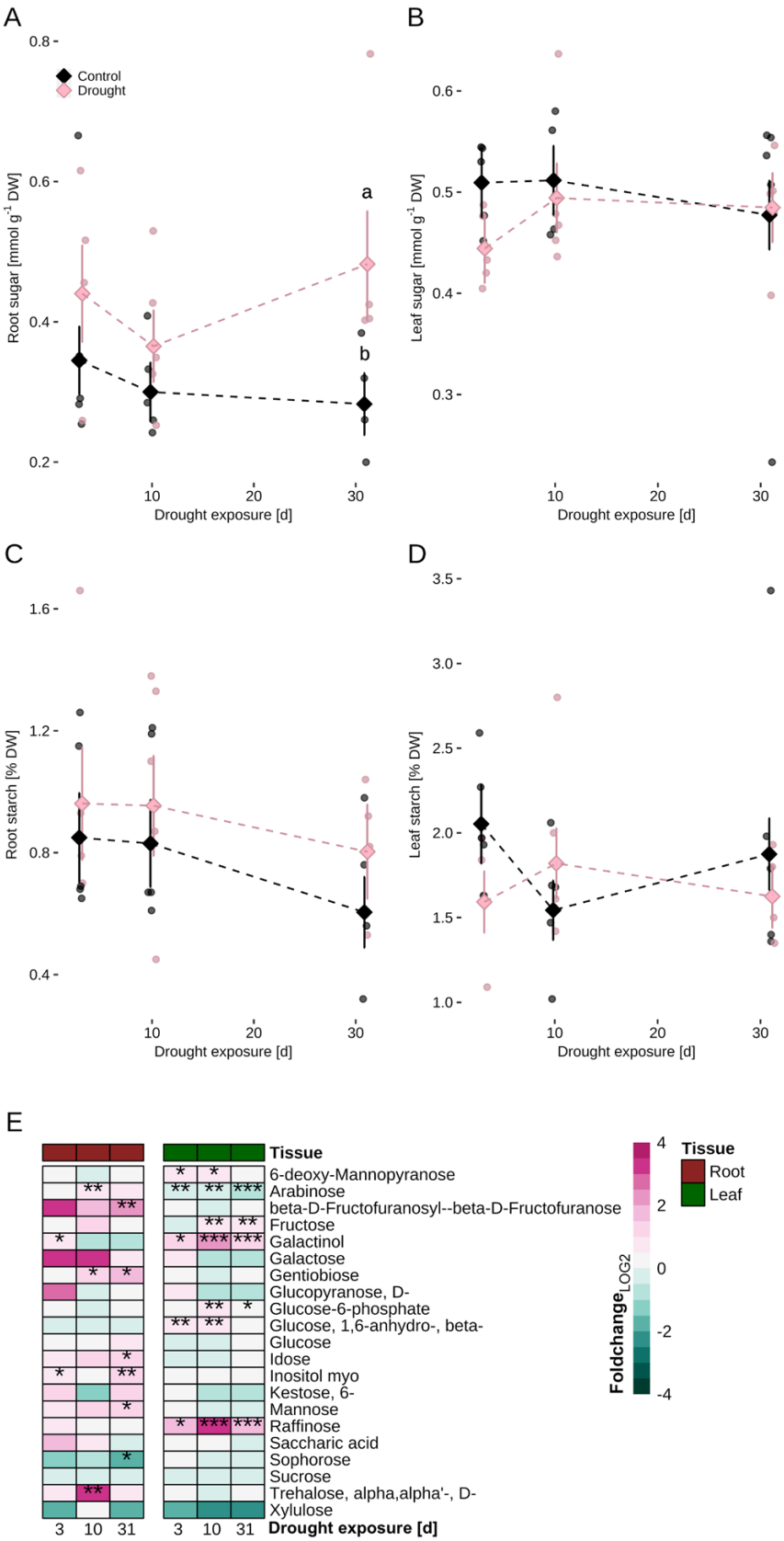

Fig. 6. Sugar concentration increases in roots of *Phoenix dactylifera* cv. Khalas after 4 weeks of drought exposure while that of leaves remains unaffected. Concentrations in roots and leaves, respectively, of soluble sugars (A) and (B), starch (C) and (D), and (E) individual changes in sugar (alcohols and derivates) levels in roots and leaves of date palms grown in phytotrons simulating Saudi Arabia summer climate conditions after 3, 10, and 31 d under well-watered (control) or drought conditions. (A–D) Means ±SE; points shown represent raw data; Tukey's, $P \leq 0.05$; different letters indicate significant differences of water regime comparison within a time point; no letters, $P > 0.05$. (E) Means of the fold-change$_{log2}$ of the relative metabolite contents are indicated by a color code. Asterisks indicate the level of significance (*$P \leq 0.05$; **$P \leq 0.01$; ***$P \leq 0.001$); n=4–5.

In roots, the amino acid composition was dominated by high concentrations of asparagine, with ~150 μmol g^{-1} DW (Fig. 7C). This concentration was similar to control conditions at 3 d and 10 d of drought. However, after 31 d, the concentration declined in the control, but remained unaffected in drought-exposed roots, resulting in an increase of ~100 μmol g^{-1} DW. Other amino acids such as proline, serine, alanine, and citrulline were among the amino acids detected, with concentrations ranging from 1 μmol g^{-1} DW to 9 μmol g^{-1} DW. Increases related to drought exposure were observed, for example with an increase of ~5 μmol g^{-1} DW for proline, serine, and alanine, while other amino acids showed lower or no drought-related increases. The amino acid composition of the leaves differed from that of the roots, primarily due to a 10-fold lower asparagine concentration, unaffected by drought (Fig. 7D). Drought exposure increased concentrations of other amino acids in leaves compared with roots, including arginine, citrulline, valine, gamma-aminobutyric acid (GABA), and proline, which showed increases of up to 4 μmol g^{-1} DW. The concentrations of valine, proline, and GABA increased transiently, reaching their peak after 10 d of drought, mirroring the total amino acid trend in leaves (Fig. 7B).

Acclimation of amino acid metabolism during long-term drought exposure

Drought-induced acclimation of amino acid metabolism was evident at the transcript and protein levels after 31 d of drought. In roots, three genes of amino acid metabolism were differentially expressed, with one down-regulated related to amino acid degradation, and two up-regulated related to the shikimate family and, thus, to the synthesis of aromatic amino acids (Supplementary Table S1G). Drought-related changes in aromatic amino acid biosynthesis were also evident at the protein level (Fig. 3A). Among the 19 proteins annotated to 'amino acid metabolic process' (GO:0006530), pyruvate decarboxylase 2 and 4, involved in aromatic amino acid catabolism, were consistently decreased (–0.5-$fold_{log2}$). Other proteins involved in aromatic amino acid metabolism such as chorismite synthase (–0.3-$fold_{log2}$), UDP-glucosyltransferase 74F2 (0.6-$fold_{log2}$), and two homologous 3-deoxy-D-arabino-heptulosonate 7-phosphate synthases (0.6-$fold_{log2}$) were differentially changed. In addition, protein levels of a glutamate synthase and two glutamine synthetases, catalyzing the conversion of glutamate to glutamine, were about halved after 31 d of drought. Proteins associated with protein biosynthesis, which play a role in the attachment of amino acids to their corresponding tRNAs, including glycyl-tRNA synthetase/glycine-tRNA ligase and tRNA synthetase class I family protein, exhibited 0.5-$fold_{log2}$ increases. In leaves, a total of 29 genes related to amino acid metabolism were differentially expressed (Supplementary Table S1G), with 17 up-regulated, mostly related to biosynthesis, and 12 down-regulated related to both biosynthesis and catabolism. No alterations in related proteins were observed following 31 d of drought exposure in comparison with the well-watered control.

Root osmotic adjustment involves accumulation of sugars and amino acids, albeit in varying amounts

To assess the contribution of the individual osmolyte compounds to the OA observed in date palm roots in response to drought exposure (Fig. 4E), individual osmolyte concentrations were correlated with their sum, all related to the water content determined in the individual tissue fractions. To overview the collinearity between the variables, the relative importance of the individual osmolytes to explain the variance in the sum of osmolytes was analyzed. In roots, the concentration of minerals contributed the most (45%), followed by sugars (39%) and amino acids (16%). This result was also reflected in the individual correlation analysis of each osmolyte (Fig. 8A, C, E), where minerals showed the highest correlation (R=0.85, P<0.001), followed by soluble sugars (R=0.79, P<0.001) and amino acids (R=0.58, P<0.001), confirming that the changes in osmotic strength were independent of the water regime and time point dominated by mineral concentrations. Comparison of the individual osmolyte contributions to the total increase in osmotic strength observed in date palm roots after 31 d of drought exposure revealed that sugars and amino acids had a significant increase of ~80 mmol l^{-1} and 40 mmol l^{-1} tissue water, respectively, compared with the well-watered controls. However, the change in mineral concentration (+40 mmol l^{-1} tissue water) was not significant. Thus, with respect to the total increase in root osmotic strength after 31 d of drought (i.e. 160 mmol l^{-1} tissue water), organic osmolytes accounted for ~75% of the osmolytes used by date palm for drought-related osmotic adjustment (Fig. 9).

In leaves, the relative importance in the regression with the sum of osmolytes was also dominated by minerals (60%), followed by sugars (39%) and amino acids (1%). These contributions were reflected in the positive correlations between total osmolyte concentration and minerals (R=0.81, P<0.001) and soluble sugars (R=0.68, P<0.001), respectively (Fig. 8B, D). However, no increase in leaf osmolyte concentration was evident after 31 d of drought (Figs 4F, 8B, D, F). Conversely, the higher mineral concentration in the leaves of well-watered plants (Fig. 8B) suggested enhanced mineral uptake, likely to be facilitated by mass flow driven by higher transpiration rates, a consequence of greater soil water availability.

Discussion

Date palm mitigates drought-related radical generation by increasing anti-oxidant activity

Date palm is an important crop that is able to survive extreme environmental conditions such as heat and drought (Arab *et al.*, 2016; Du *et al.*, 2019; Kruse *et al.*, 2019); however, date palm productivity and fruit quality are challenged by drought (Allbed *et al.*, 2017; Ali-Dinar *et al.*, 2023), emphasizing the need for a better understanding of date palm drought

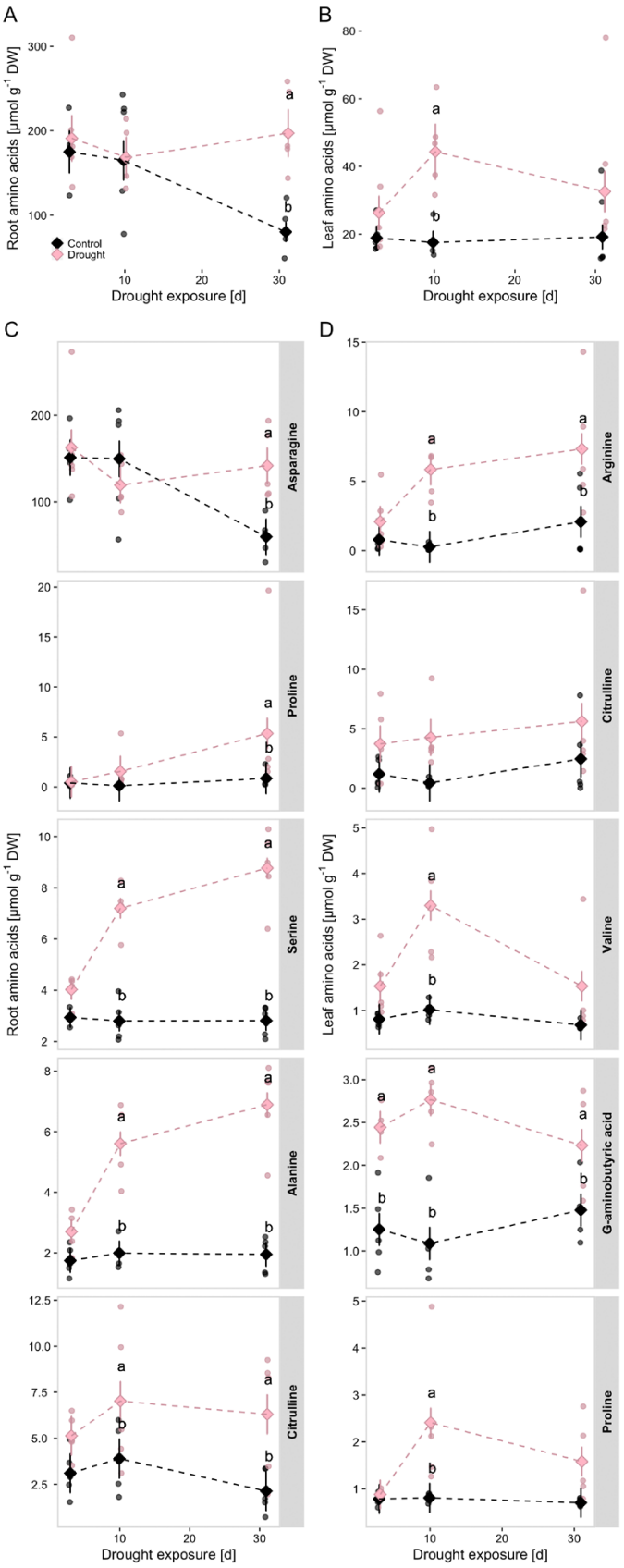

Fig. 7. Amino acid concentration increases in roots of *Phoenix dactylifera* cv. Khalas already after 10 d of drought exposure. Total concentration of amino acids in (A) root and (B) leaf and the top five individual amino acids with highest contributions to total amino acid accumulation under drought exposure in (C) roots and (D) leaves of date palms grown in phytotrons simulating Saudi Arabia summer climate conditions after 3, 10, and 31 d under well-watered (control) or drought conditions. Means ±SE. Points shown represent raw data; n=5; Tukey's, $P \leq 0.05$; different letters indicate significant differences in water regime comparisons within a time point; no letters, $P > 0.05$. Individual amino acids were selected according to the highest positive delta to the well-watered controls at the peak of accumulation (Supplementary Fig. S2); a full list of all amino acids detected is provided in Supplementary Fig. S3. Color code as in (A) for all panels.

acclimation. To investigate the early metabolic acclimation to drought with a focus on OA, we analyzed date palms exposed to a 1 month period of drought. In response to these harsh environmental conditions, date palm shoot growth was significantly arrested (Fig. 4B), resembling previous observations of reduced leaf growth under field conditions (Ali-Dinar *et al.*, 2023). Reduced shoot growth under drought is attributed to diminished photoassimilation observed in drought-exposed date palms (Kruse *et al.*, 2019; Alhajhoj *et al.*, 2022), which disproportionately affects the canopy compared with the roots, and reduces water potential in expanding leaf cells. These factors drive an increased root-to-shoot ratio (Davies, 2006), enabling greater resource allocation to root development, enhancing the ability of the plant to explore deeper soil layers for water uptake. However, as date palm is a relatively slow growing species, the root growth stimulation was not pronounced (Fig. 4A) during the relatively short 1 month experimental period.

Consistent with the observed shoot growth arrest, the drought-inducible stress hormone ABA, a negative regulator of plant growth (Yao and Finlayson, 2015) and stomatal opening (Müller *et al.*, 2017), accumulated in both roots and leaves from the third day of drought exposure (Fig. 1). This pattern was also evident for JA-Ile, which is involved in stress acclimation (Riemann *et al.*, 2015) and required for ABA biosynthesis in drought-exposed roots (de Ollas and Dodd, 2016). In line with this, JA-Ile remained constantly elevated in drought-exposed date palm roots. In leaves, however, JA-Ile decreased after 10 d of drought exposure, despite increased ROS, which can stimulate JA signaling (Ismail *et al.*, 2014). As a result of continuous stomatal closure and, thus, reduced leaf gas exchange and transpirational cooling, increasing leaf temperature and negative redox potential might cause generation of ROS (Rennenberg *et al.*, 2006; Lee *et al.*, 2012). This was evident in the leaves of date palm by increased levels of ROS (H_2O_2) (Fig. 2), as observed previously in date palms exposed to drought and heat (Arab *et al.*, 2016; Du *et al.*, 2019) or salt (Mueller *et al.*, 2023). Consistently, date palm increased anti-oxidant activity as evidenced by the increased abundance (Fig. 3) and activity of metabolites and enzymes involved in the Foyer–Halliwell–Asada cycle (Fig. 2) (Du *et al.*, 2024), indicating a continued need to balance the cellular ROS homeostasis (Noctor *et al.*, 2016) under drought.

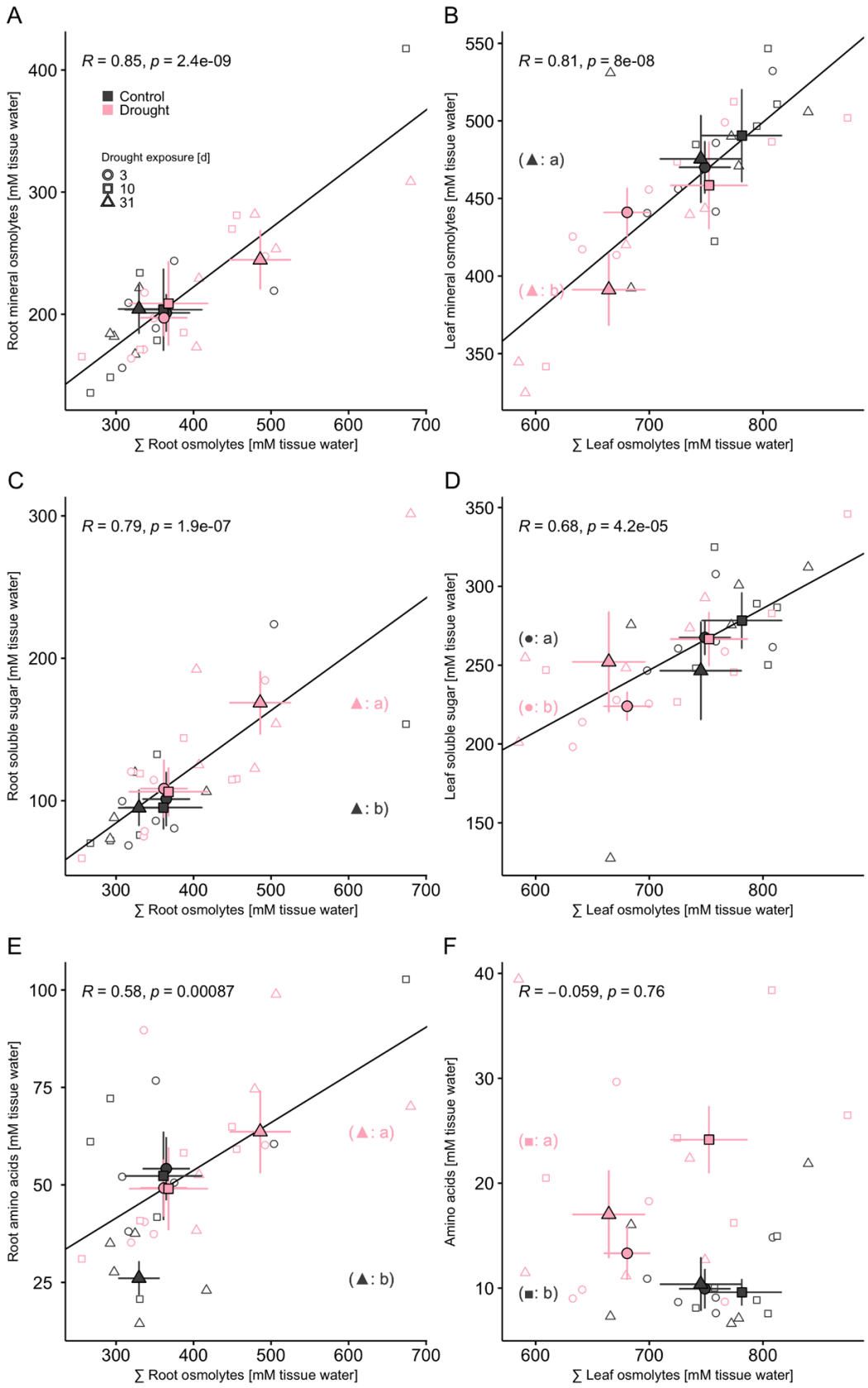

Fig. 8. Total osmolyte concentration in roots of *Phoenix dactylifera* cv. Khalas increases with minerals, soluble sugars, and amino acids. Correlation of the sum of measured osmolyte concentrations with concentrations of minerals (A) and (B), sugars (C) and (D), and amino acids (E) and (F) in roots and

leaves, respectively, of date palms grown in phytotrons simulating Saudi Arabia summer climate conditions after 3, 10, and 31 d under well-watered (control) or drought conditions. Measured osmolyte concentrations were related to cellular hydration of individual date palms. Pearson's regression based on the raw data shown as open symbols; filled symbols represent means ±SE; n=5; Tukey's, $P \leq 0.05$; different letters in parentheses indicate significant differences of individual osmolyte concentrations with respect to comparison of water regimes within a time point that is indicated by the shape code; no letters, $P > 0.05$. Shape and color codes as for (A) for all panels.

Photosynthetic acclimation to drought involves stabilization and restructuring of antennae and lipid composition

Water deficit represents a significant challenge to photosynthesis, decreasing photosynthetic performance, while increasing the risk of ROS generation and oxidative damage to the photosynthetic apparatus (Pandey *et al.*, 2023). Consistently, several changes in relation to the stabilization of the photosynthetic apparatus were evident in date palm leaves following 1 month drought exposure, with prominent increases of chaperons (Fig. 3B), such as

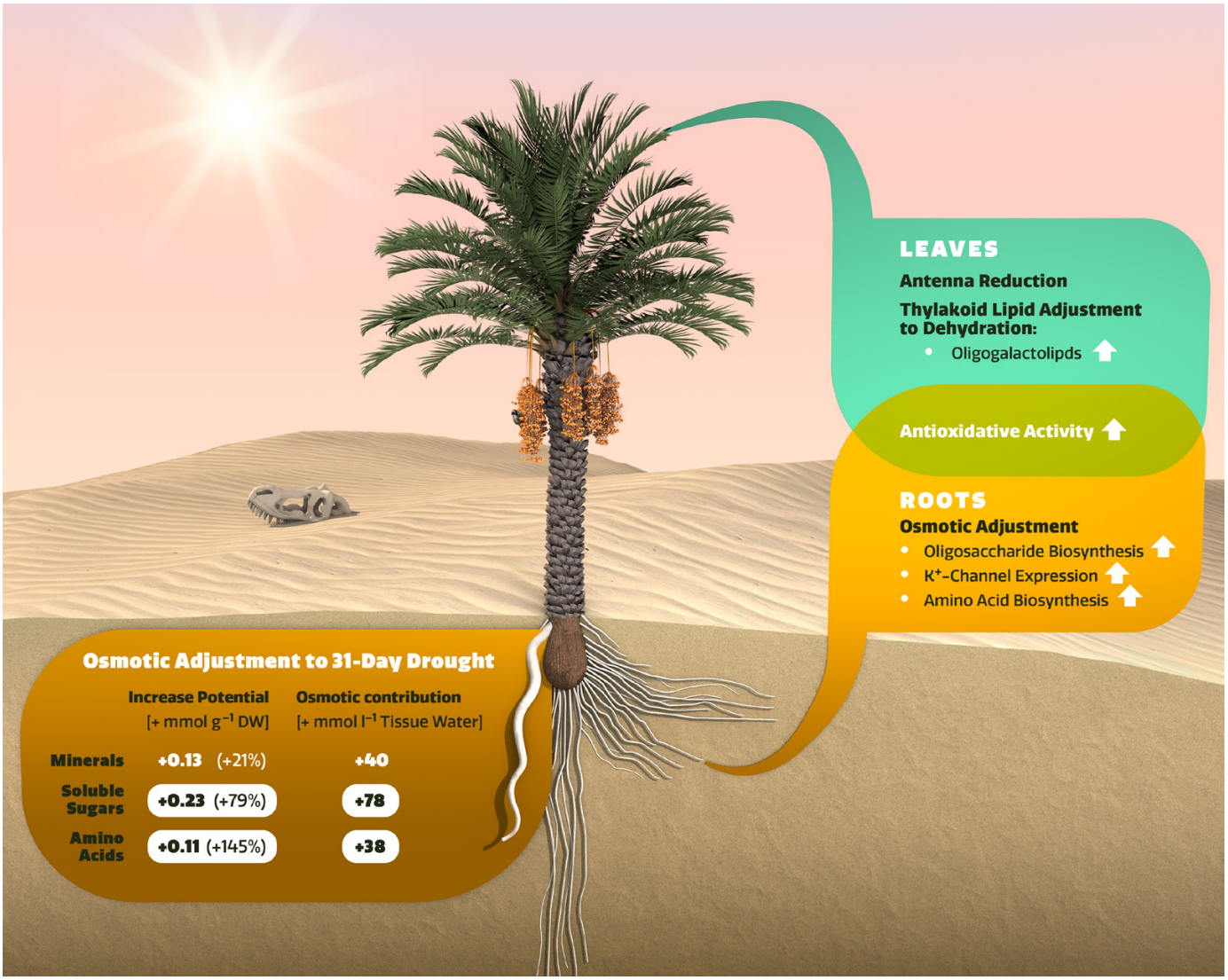

Fig. 9. Early acclimation of date palm (*Phoenix dactylifera* L.) to desert drought. Leaf acclimation includes a remodeling of thylakoid lipid composition together with a restructuring of the photosynthetic apparatus (i.e. a reduction of antennae), both of which prevent the formation of reactive oxygen species (ROS). In leaves and roots, oxidative damage resulting from increased ROS formation is counteracted by increased activity of the anti-oxidant machinery. Roots adapt osmotically to water deficit by accumulating both mineral and organic osmolytes, with organic osmolytes accounting for ~75% of the increase in osmotic strength. Oligosaccharide and amino acid biosynthesis are stimulated, fueling the accumulation of organic osmolytes. Significant increases in osmolytes after 31 d of drought, shown as a difference from the well-watered controls, are highlighted with a white background (Tukey's, $P \leq 0.05$).

chaperonin 60 (Holland *et al.*, 1998) and HSP70 (Aghaie and Tafreshi, 2020), that stabilize photosystems and support chloroplast differentiation from plastids under elevated temperatures (Kim and An, 2013). Consistent with previous observations (Ghirardo *et al.*, 2021), constituents of photosystem antennae such as Chl *a*/*b*-binding proteins (CBPs) were also increased, indicating a drought-related modification (i.e. reduction) of antenna complexes that might prevent production of ROS by excess light-harvesting activity (Du *et al.*, 2018). Moreover, CBPs play a role in plant acclimation to environmental cues (Ganeteg *et al.*, 2004), for example in enhancing stomatal sensitivity to ABA (Xu *et al.*, 2012; Liu *et al.*, 2013). Thus, the increase of CBPs in date palm leaves might also be an acclimatory response to enhance guard cell ABA sensitivity to avoid transpirational water loss. Drought-induced acclimation in the photosynthetic apparatus was also reflected in remodeling of the thylakoid membrane. This was suggested by changed lipid metabolism, favoring an increased poly- to monogalactolipid ratio (Supplementary Table S1C). This remodeling is relevant for avoiding membrane distortion and fusion during desiccation (Chng *et al.*, 2022). This maintains the integrity of grana stacks (Kobayashi, 2016), which are susceptible to disruption under low cellular water conditions (Yu *et al.*, 2021), ultimately impeding photosynthesis. The disassembly of monogalactolipids from thylakoid membranes (Young *et al.*, 2022) and the removal of excess lipids from membranes during desiccation-induced organelle shrinkage (Gasulla *et al.*, 2013) might account for the suggested increase in TAG synthesis (Supplementary Table S1C). This process could also help sequester toxic lipid intermediates that accumulate due to membrane lipid remodeling (Lu *et al.*, 2020). The combined remodeling of thylakoid membranes and the restructuring of the photosynthetic apparatus might underlie the previously observed drought acclimation of date palm photosynthesis, namely the reduction in electron transport rate at reduced photosynthetic carbon fixation (Kruse *et al.*, 2019; Ghirardo *et al.*, 2021), with reduced risk of photooxidative damage (Mäkelä, 1996; Kruse *et al.*, 2019).

Organic osmolytes make a major contribution to the early osmotic adjustment of roots to drought

In addition to stomatal closure, ABA accumulation also leads to various acclimatory responses involved in stress mitigation (Yoshida *et al.*, 2014), such as OA (Shabala and Shabala, 2011). Because root cells contain more water per dry mass than leaves (Fig. 4C, D), OA of roots requires more osmolytes and, thus, is energetically more demanding (Munns *et al.*, 2020). Accordingly, drought-related osmolyte accumulation was more pronounced in date palm roots than in leaves. In roots, a modest accumulation of the energetically cheap mineral osmolyte K^+ was detected (Raven, 1985; Shabala and Shabala, 2011; Munns *et al.*, 2020). However, the contribution of mineral osmolytes (~40 mM) to OA after the 31 d drought was relatively minor compared with the significant role of expensive organic osmolytes, which accounted for 75% of the total increase in root osmotic strength (Fig. 9). Consistent with the known pattern that drought stress leads to a rapid increase in soluble sugars to minimize dehydration damage (Kaiser, 1987; Slama *et al.*, 2015; Fàbregas and Fernie, 2019), date palm accumulated soluble sugars in the roots following drought exposure (Safronov *et al.*, 2017; Anli *et al.*, 2020), with the highest increase of 80 mM (Fig. 8) among the analyzed osmolytes. Consistently, roots showed marked up-regulation of galactinol and stachyose synthases involved in oligosaccharide biosynthesis (Li et al., 2020). Numerous sugars other than the typical free sugars, such as sucrose, glucose, and fructose (Fàbregas and Fernie, 2019), accumulated in roots (Fig. 6E), including gentiobiose, idose, myo-inositol, mannose, and the non-reducing disaccharide trehalose, a highly soluble and unreactive sugar that accumulates in desiccation-tolerant species during dehydration (Illhan *et al.*, 2015). Temporary increases in gentiobiose and trehalose were also observed in date palms exposed to hyperosmotic salt conditions. However, the total amount of sugars only increased slightly (Al Kharusi *et al.*, 2019) or remained unaffected in date palms exposed to salinity (Mueller *et al.*, 2023), similar to salt-exposed barley, where sugars also modestly contributed to OA (Annunziata *et al.*, 2016). These findings suggest that the remarkable accumulation of soluble sugars with the underlying reprogramming of carbohydrate metabolism in the roots of date palm represents an acclimatory response specific to drought.

The amino acid contribution of ~40 mM to drought-related OA in roots (Fig. 8E) was about half that of sugars (Fig. 9). The often accumulating compatible osmolyte proline (Slama *et al.*, 2015) was not among the major contributors. Instead, the increase was mainly due to the generally high concentrations of asparagine in date palm roots. Asparagine can serve as a storage compound for assimilated nitrogen due to its high nitrogen to carbon ratio and might accumulate, for example, in response to stress-related reduction in protein biosynthesis (Lea *et al.*, 2007). In date palm (Yaish, 2015; Safronov *et al.*, 2017; Shareef *et al.*, 2020; Du *et al.*, 2021) and other halophytes (Slama *et al.*, 2015), free amino acids accumulate under drought. This accumulation can be a consequence of numerous factors such as water deficit and ABA-related protein degradation (Huang and Jander, 2017). However, concentrations of soluble proteins were previously shown not to be affected by drought (Du *et al.*, 2023), suggesting no excessive drought-related protein degradation. Therefore, the observed stimulation of amino acid metabolism during drought strengthens the argument that amino acids might act as a metabolic cache for organic nitrogen under stress also in date palm (Hildebrandt, 2018), which in parallel provides a significant contribution to OA in the early drought acclimation of date palm.

Date palm does not preferentially use cheap mineral osmolytes for osmotic adjustment in early drought acclimation

Halophytes such as date palm are thought to tolerate higher cellular mineral concentrations (Flowers *et al.*, 2015). Therefore,

OA could be achieved primarily through the use of mineral osmolytes with low risk of ion toxicity. This trait might be exploited to achieve cost-effective OA through mineral uptake and sequestration (Shabala and Shabala, 2011; Munns *et al.*, 2020), while reducing the need to synthesize organic compounds and divert them from growth. Date palm has been shown to remarkably control the uptake and long-distance transport of Na^+ and Cl^- while promoting the uptake of K^+ when growing in a hyperosmotic saline environment (Mueller *et al.*, 2023). However, despite a marginal increase of K^+ in roots, date palm showed no extensive mineral use for OA in early drought acclimation, while significant amounts of sugars and amino acids were diverted from maintenance and growth. This result confirms the primary use of organic osmolytes for drought-related OA (Munns *et al.*, 2020) in the early acclimation of date palm to drought, although increased uptake and sequestration of energetically less expensive mineral osmolytes would be a strategy preventing stress-induced growth arrest due to energy limitation (Shabala and Shabala, 2011; Munns *et al.*, 2020). Drought acclimation and the role of osmolytes in osmotic adjustment over a full phenological season warrant further investigation to determine if prolonged drought reduces the contribution of organic osmolytes to OA, thereby reallocating resources towards root growth to access deeper water layers.

Conclusion

Date palm is a useful non-model crop species for studying tolerance to extreme environments, owing to its remarkable resilience to high salinity and drought. It is able to survive in arid deserts because it (i) restructures the photosynthetic apparatus to avoid formation of ROS; (ii) promotes anti-oxidative metabolism; and (iii) osmotically adjusts the roots to low soil water potential. Energetically expensive organic osmolytes are essential for osmotic adjustment. Halophytes, with their expected higher intrinsic tissue tolerance, could achieve osmotic adjustment mainly by using mineral osmolytes with less risk of ion toxicity. In contrast to this assumption, date palm relies on sugars and amino acids rather than promoting mineral uptake in the early acclimation to drought. This strategy might bind resources to the detriment of growth and maintenance processes.

Supplementary data

The following supplementary data are available at *JXB* online.

Table S1. Transcriptomic response of leaves and roots of date palm cv. Khalas after 31 d under well-watered or drought conditions.

Table S2. Proteomic response of leaves and roots of date palm cv. Khalas after 31 d under well-watered or drought conditions.

Fig. S1. Mineral concentrations in leaves and roots after 3, 10, and 31 d under well-watered or drought conditions in date palm cv. Khalas.

Fig. S2. Amino acid contribution to increase in total amino acid concentration in response to drought in date palm cv. Khalas.

Fig. S3. Amino acid concentrations leaves and roots after 3, 10, and 31 d under well-watered or drought conditions in date palm cv. Khalas.

Acknowledgements

In Memoriam of Professor Philip J. White (1960–2023) and Professor Jaakko Kangasjärvi (1960–2024).

Author contributions

BLF, MM, HMM, BD, TL, SCC, PW, MR, AM, JBW, J-PS, C-MG, and PA: performed the research and analyzed the data; J-PS, KFXM, JKu, JKa, HR, C-MG, PA, and RH: designed the study; BLF: wrote the draft of the manuscript with input from MM, PA, C-MG, and HR, which was revised by all the authors.

Conflict of interest

The authors declare that they have no known competing financial interests or personal relationships that could have appeared to influence the work reported in this paper.

Funding

PW, KFXM, JKu, JKa, HR, and RH were supported by grants from the King Saud University, Riyadh, Saudi Arabia. MM was funded by the German Research Foundation (DFG) - TRR 356. C-MG was funded by the German Research Foundation (DFG) - Projektnummer 499216091.

Data availability

RNA-seq data available in ArrayExpress (https://www.ebi.ac.uk/fg/annotare) under accession number E-MTAB-14123 and are available with the proteomic data in the Supplementary data. Additional data supporting the findings of this study are available from the corresponding authors upon request.

References

Aghaie P, Tafreshi SAH. 2020. Central role of 70-kDa heat shock protein in adaptation of plants to drought stress. Cell Stress & Chaperones **25**, 1071–1081.

Alhajhoj MR, Munir M, Sudhakar B, Ali-Dinar HM, Iqbal Z. 2022. Common and novel metabolic pathways related ESTs were upregulated in three date palm cultivars to ameliorate drought stress. Scientific Reports **12**, 15027.

Ali U, Li H, Wang X, Guo L. 2018. Emerging roles of sphingolipid signaling in plant response to biotic and abiotic stresses. Molecular Plant **11**, 1328–1343.

Ali-Dinar H, Munir M, Mohammed M. 2023. Drought-tolerance screening of date palm cultivars under water stress conditions in arid regions. Agronomy **13**, 2811.

Al Kharusi L, Sunkar R, Al-Yahyai R, Yaish MW. 2019. Comparative water relations of two contrasting date palm genotypes under salinity. International Journal of Agronomy **2019**, 1–16.

Allbed A, Kumar L, Shabani F. 2017. Climate change impacts on date palm cultivation in Saudi Arabia. The Journal of Agricultural Science **155**, 1203–1218.

Amin MT, Mahmoud SH, Alazba AA. 2016. Observations, projections and impacts of climate change on water resources in Arabian Peninsula: current and future scenarios. Environmental Earth Sciences **75**, 864.

Anli M, Baslam M, Tahiri A, *et al*. 2020. Biofertilizers as strategies to improve photosynthetic apparatus, growth, and drought stress tolerance in the date palm. Frontiers in Plant Science **11**, 516818.

Annunziata MG, Ciarmiello LF, Woodrow P, Maximova E, Fuggi A, Carillo P. 2016. Durum wheat roots adapt to salinity remodeling the cellular content of nitrogen metabolites and sucrose. Frontiers in Plant Science **7**, 2035.

Arab L, Kreuzwieser J, Kruse J, Zimmer I, Ache P, Alfarraj S, Al-Rasheid KAS, Schnitzler J-P, Hedrich R, Rennenberg H. 2016. Acclimation to heat and drought—lessons to learn from the date palm (*Phoenix dactylifera*). Environmental and Experimental Botany **125**, 20–30.

Blum A. 2017. Osmotic adjustment is a prime drought stress adaptive engine in support of plant production. Plant, Cell & Environment **40**, 4–10.

Bolger AM, Lohse M, Usadel B. 2014. Trimmomatic: a flexible trimmer for Illumina sequence data. Bioinformatics **30**, 2114–2120.

Boyle RKA, McAinsh M, Dodd IC. 2016. Stomatal closure of *Pelargonium* × *hortorum* in response to soil water deficit is associated with decreased leaf water potential only under rapid soil drying. Physiologia Plantarum **156**, 84–96.

Bray NL, Pimentel H, Melsted P, Pachter L. 2016. Near-optimal probabilistic RNA-seq quantification. Nature Biotechnology **34**, 525–527.

Brunner I, Herzog C, Dawes MA, Arend M, Sperisen C. 2015. How tree roots respond to drought. Frontiers in Plant Science **6**, 547.

Buts K, Michielssens S, Hertog MLATM, Hayakawa E, Cordewener J, America AHP, Nicolai BM, Carpentier SC. 2014. Improving the identification rate of data independent label-free quantitative proteomics experiments on non-model crops: a case study on apple fruit. Journal of Proteomics **105**, 31–45.

Carpentier SC, Witters E, Laukens K, Deckers P, Swennen R, Panis B. 2005. Preparation of protein extracts from recalcitrant plant tissues: an evaluation of different methods for two-dimensional gel electrophoresis analysis. Proteomics **5**, 2497–2507.

Chaves M, Davies B. 2010. Drought effects and water use efficiency: improving crop production in dry environments. Functional Plant Biology **37**, iii–vi.

Chen THH, Murata N. 2011. Glycinebetaine protects plants against abiotic stress: mechanisms and biotechnological applications. Plant, Cell & Environment **34**, 1–20.

Chng C-P, Wang K, Ma W, Hsia KJ, Huang C. 2022. Chloroplast membrane lipid remodeling protects against dehydration by limiting membrane fusion and distortion. Plant Physiology **188**, 526–539.

Cornic G, Briantais JM. 1991. Partitioning of photosynthetic electron flow between CO_2 and O_2 reduction in a C3 leaf (*Phaseolus vulgaris* L.) at different CO_2 concentrations and during drought stress. Planta **183**, 178–184.

Davies WJ. 2006. Responses of plant growth and functioning to changes in water supply in a changing climate. In: Morison JI, Morecroft MD. eds. Plant growth and climate change. Chichester, UK: Wiley, 96–117.

Dávila-Lara A, Rahman-Soad A, Reichelt M, Mithöfer A. 2021. Carnivorous *Nepenthes* × *ventrata* plants use a naphthoquinone as phytoanticipin against herbivory. PLoS One **16**, e0258235.

de Mendiburu F. 2019. Package 'agricolae'. https://CRAN.R-project.org/package=agricolae.

de Ollas C, Dodd IC. 2016. Physiological impacts of ABA–JA interactions under water-limitation. Plant Molecular Biology **91**, 641–650.

Dodd IC, Egea G, Davies WJ. 2008. Abscisic acid signalling when soil moisture is heterogeneous: decreased photoperiod sap flow from drying roots limits abscisic acid export to the shoots. Plant, Cell & Environment **31**, 1263–1274.

Döring J, Will F, Löhnertz O, Krause B, Kauer R. 2022. The impact of sustainable management regimes on amino acid profiles in grape juice, grape skin flavonoids and hydroxycinnamic acids. OENO One **56**, 319–333.

Du B, Haensch R, Alfarraj S, Rennenberg H. 2024. Strategies of plants to overcome abiotic and biotic stresses. Biological Reviews of the Cambridge Philosophical Society **99**, 1524–1536.

Du B, Kruse J, Winkler JB, Alfarraj S, Albasher G, Schnitzler J-P, Ache P, Hedrich R, Rennenberg H. 2021. Metabolic responses of date palm (*Phoenix dactylifera* L.) leaves to drought differ in summer and winter climate. Tree Physiology **41**, 1685–1700.

Du B, Kruse J, Winkler JB, Alfarray S, Schnitzler J-P, Ache P, Hedrich R, Rennenberg H. 2019. Climate and development modulate the metabolome and antioxidative system of date palm leaves. Journal of Experimental Botany **70**, 5959–5969.

Du B, Winkler JB, Ache P, White PJ, Dannenmann M, Alfarraj S, Albasher G, Schnitzler J-P, Hedrich R, Rennenberg H. 2023. Differences of nitrogen metabolism in date palm (*Phoenix dactylifera*) seedlings subjected to water deprivation and salt exposure. Tree Physiology **43**, 587–596.

Du Z-Y, Lucker BF, Zienkiewicz K, Miller TE, Zienkiewicz A, Sears BB, Kramer DM, Benning C. 2018. Galactoglycerolipid lipase PGD1 is involved in thylakoid membrane remodeling in response to adverse environmental conditions in Chlamydomonas. The Plant Cell **30**, 447–465.

Fàbregas N, Fernie AR. 2019. The metabolic response to drought. Journal of Experimental Botany **70**, 1077–1085.

Fan J, Zhai Z, Yan C, Xu C. 2015. Arabidopsis TRIGALACTOSYLDIACYLGLYCEROL5 interacts with TGD1, TGD2, and TGD4 to facilitate lipid transfer from the endoplasmic reticulum to plastids. The Plant Cell **27**, 2941–2955.

Finkelstein RR, Gampala SSL, Rock CD. 2002. Abscisic acid signaling in seeds and seedlings. The Plant Cell **14 Suppl14**, S15–S45.

Flowers TJ, Munns R, Colmer TD. 2015. Sodium chloride toxicity and the cellular basis of salt tolerance in halophytes. Annals of Botany **115**, 419–431.

Fricke W. 2020. Energy costs of salinity tolerance in crop plants: night-time transpiration and growth. New Phytologist **225**, 1152–1165.

Ganeteg U, Külheim C, Andersson J, Jansson S. 2004. Is each light-harvesting complex protein important for plant fitness? Plant Physiology **134**, 502–509.

Gasulla F, vom Dorp K, Dombrink I, Zähringer U, Gisch N, Dörmann P, Bartels D. 2013. The role of lipid metabolism in the acquisition of desiccation tolerance in *Craterostigma plantagineum*: a comparative approach. The Plant Journal **75**, 726–741.

Ghirardo A, Nosenko T, Kreuzwieser J, *et al*. 2021. Protein expression plasticity contributes to heat and drought tolerance of date palm. Oecologia **197**, 903–919.

Golldack D, Lüking I, Yang O. 2011. Plant tolerance to drought and salinity: stress regulating transcription factors and their functional significance in the cellular transcriptional network. Plant Cell Reports **30**, 1383–1391.

Grömping U. 2007. Relative importance for linear regression in R: the package relaimpo. Journal of Statistical Software **17**, 1–27.

Haas BJ, Papanicolaou A, Yassour M, *et al*. 2013. De novo transcript sequence reconstruction from RNA-seq using the Trinity platform for reference generation and analysis. Nature Protocols **8**, 1494–1512.

Hama H. 2010. Fatty acid 2-hydroxylation in mammalian sphingolipid biology. Biochimica et Biophysica Acta **1801**, 405–414.

Hatanaka T, Tomita Y, Matsuoka D, Sasayama D, Fukayama H, Azuma T, Soltani Gishini MF, Hildebrand D. 2022. Different acyl-CoA:diacylglycerol acyltransferases vary widely in function, and a targeted amino acid substitution enhances oil accumulation. Journal of Experimental Botany **73**, 3030–3043.

Hildebrandt TM. 2018. Synthesis versus degradation: directions of amino acid metabolism during Arabidopsis abiotic stress response. Plant Molecular Biology **98**, 121–135.

Holland N, Belkind A, Holland D, Pick U, Edelman M. 1998. Stress-responsive accumulation of plastid chaperonin 60 during seedling development. The Plant Journal **13**, 311–316.

Huang T, Jander G. 2017. Abscisic acid-regulated protein degradation causes osmotic stress-induced accumulation of branched-chain amino acids in *Arabidopsis thaliana*. Planta **246**, 737–747.

Hummel J, Strehmel N, Selbig J, Walther D, Kopka J. 2010. Decision tree supported substructure prediction of metabolites from GC-MS profiles. Metabolomics **6**, 322–333.

Ilhan S, Ozdemir F, Bor M. 2015. Contribution of trehalose biosynthetic pathway to drought stress tolerance of *Capparis ovata* Desf. Plant Biology (Stuttgart, Germany) **17**, 402–407.

Ingram J, Bartels D. 1996. The molecular basis of dehydration tolerance in plants. Annual Review of Plant Physiology and Plant Molecular Biology **47**, 377–403.

Ismail A, Takeda S, Nick P. 2014. Life and death under salt stress: same players, different timing? Journal of Experimental Botany **65**, 2963–2979.

Jin Y, Yuan Y, Gao L, Sun R, Chen L, Li D, Zheng Y. 2017. Characterization and functional analysis of a type 2 diacylglycerol acyltransferase (DGAT2) gene from oil palm (*Elaeis guineensis* Jacq.) mesocarp in *Saccharomyces cerevisiae* and transgenic *Arabidopsis thaliana*. Frontiers in Plant Science **8**, 1791.

Kaiser WM. 1987. Effects of water deficit on photosynthetic capacity. Physiologia Plantarum **71**, 142–149.

Kim S-R, An G. 2013. Rice chloroplast-localized heat shock protein 70, OsHsp70CP1, is essential for chloroplast development under high-temperature conditions. Journal of Plant Physiology **170**, 854–863.

Kobayashi K. 2016. Role of membrane glycerolipids in photosynthesis, thylakoid biogenesis and chloroplast development. Journal of Plant Research **129**, 565–580.

Kolde R. 2015. Package 'pheatmap'. https://CRAN.R-project.org/package=pheatmap.

Kreuzwieser J, Hauberg J, Howell KA, Carroll A, Rennenberg H, Millar AH, Whelan J. 2009. Differential response of gray poplar leaves and roots underpins stress adaptation during hypoxia. Plant Physiology **149**, 461–473.

Kruse J, Adams M, Winkler B, Ghirardo A, Alfarraj S, Kreuzwieser J, Hedrich R, Schnitzler J-P, Rennenberg H. 2019. Optimization of photosynthesis and stomatal conductance in the date palm *Phoenix dactylifera* during acclimation to heat and drought. New Phytologist **223**, 1973–1988.

Lea PJ, Sodek L, Parry M, Shewry PR, Halford NG. 2007. Asparagine in plants. Annals of Applied Biology **150**, 1–26.

Lee S, Seo PJ, Lee H-J, Park C-M. 2012. A NAC transcription factor NTL4 promotes reactive oxygen species production during drought-induced leaf senescence in Arabidopsis. The Plant Journal **70**, 831–844.

Li M-H, Cherubini P, Dobbertin M, Arend M, Xiao W-F, Rigling A. 2013. Responses of leaf nitrogen and mobile carbohydrates in different Quercus species/provenances to moderate climate changes. Plant Biology **15**, 177–184.

Li T, Zhang Y, Liu Y, *et al*. 2020. Raffinose synthase enhances drought tolerance through raffinose synthesis or galactinol hydrolysis in maize and Arabidopsis plants. Journal of Biological Chemistry **295**, 8064–8077.

Liu Q, Siloto RMP, Lehner R, Stone SJ, Weselake RJ. 2012. Acyl-CoA:diacylglycerol acyltransferase: molecular biology, biochemistry and biotechnology. Progress in Lipid Research **51**, 350–377.

Liu R, Xu Y-H, Jiang S-C, *et al*. 2013. Light-harvesting chlorophyll a/b-binding proteins, positively involved in abscisic acid signalling, require a transcription repressor, WRKY40, to balance their function. Journal of Experimental Botany **64**, 5443–5456.

Lu J, Xu Y, Wang J, Singer SD, Chen G. 2020. The role of triacylglycerol in plant stress response. Plants **9**, 472.

Ma W, Liu Z, Beier S, Houben A, Carpentier S. 2021. Identification of rye B chromosome-associated peptides by mass spectrometry. New Phytologist **230**, 2179–2185.

Mäkelä A. 1996. Optimal control of gas exchange during drought: theoretical analysis. Annals of Botany **77**, 461–468.

Medrano H, Escalona JM, Bota J, Gulías J, Flexas J. 2002. Regulation of photosynthesis of C3 plants in response to progressive drought: stomatal conductance as a reference parameter. Annals of Botany **89**, 895–905.

Mueller HM, Franzisky BL, Messerer M, *et al*. 2023. Integrative multi-omics analyses of date palm (*Phoenix dactylifera*) roots and leaves reveal how the halophyte land plant copes with sea water. The Plant Genome **17**, e20372.

Müller HM, Schäfer N, Bauer H, *et al*. 2017. The desert plant *Phoenix dactylifera* closes stomata via nitrate-regulated SLAC1 anion channel. New Phytologist **216**, 150–162.

Munns R, James RA, Gilliham M, Flowers TJ, Colmer TD. 2016. Tissue tolerance: an essential but elusive trait for salt-tolerant crops. Functional Plant Biology **43**, 1103–1113.

Munns R, Millar AH. 2023. Seven plant capacities to adapt to abiotic stress. Journal of Experimental Botany **74**, 4308–4323.

Munns R, Passioura JB, Colmer TD, Byrt CS. 2020. Osmotic adjustment and energy limitations to plant growth in saline soil. New Phytologist **225**, 1091–1096.

Noctor G, Mhamdi A, Foyer CH. 2016. Oxidative stress and antioxidative systems: recipes for successful data collection and interpretation. Plant, Cell & Environment **39**, 1140–1160.

Osaki M, Shinano T, Tadano T. 1991. Redistribution of carbon and nitrogen compounds from the shoot to the harvesting organs during maturation in field crops. Soil Science and Plant Nutrition **37**, 117–128.

Pandey J, Devadasu E, Saini D, Dhokne K, Marriboina S, Raghavendra AS, Subramanyam R. 2023. Reversible changes in structure and function of photosynthetic apparatus of pea (*Pisum sativum*) leaves under drought stress. The Plant Journal **113**, 60–74.

Polle A, Chakrabarti K, Schürmann W, Renneberg H. 1990. Composition and properties of hydrogen peroxide decomposing systems in extracellular and total extracts from needles of Norway spruce (*Picea abies* L., Karst.). Plant Physiology **94**, 312–319.

Puértolas J, Larsen EK, Davies WJ, Dodd IC. 2017. Applying 'drought' to potted plants by maintaining suboptimal soil moisture improves plant water relations. Journal of Experimental Botany **68**, 2413–2424.

Raven JA. 1985. Tansley review no. 2: regulation of pH and generation of osmolarity in vascular plants: a cost-benefit analysis in relation to efficiency of use of energy, nitrogen and water. New Phytologist **101**, 25–77.

R Core Team. 2013. R: a language and environment for statistical computing. Vienna, Austria: R Foundation for Statistical Computing.

Rennenberg H, Loreto F, Polle A, Brilli F, Fares S, Beniwal RS, Gessler A. 2006. Physiological responses of forest trees to heat and drought. Plant Biology **8**, 556–571.

Riemann M, Dhakarey R, Hazman M, Miro B, Kohli A, Nick P. 2015. Exploring jasmonates in the hormonal network of drought and salinity responses. Frontiers in Plant Science **6**, 1077.

Robinson MD, McCarthy DJ, Smyth GK. 2010. edgeR: a Bioconductor package for differential expression analysis of digital gene expression data. Bioinformatics (Oxford, England) **26**, 139–140.

Ryan AC, Hewitt CN, Possell M, Vickers CE, Purnell A, Mullineaux PM, Davies WJ, Dodd IC. 2014. Isoprene emission protects photosynthesis but reduces plant productivity during drought in transgenic tobacco (*Nicotiana tabacum*) plants. New Phytologist **201**, 205–216.

Safronov O, Kreuzwieser J, Haberer G, *et al*. 2017. Detecting early signs of heat and drought stress in *Phoenix dactylifera* (date palm). PLoS One **12**, e0177883.

Saharwardi MS, Dasari HP, Aggarwal V, Ashok K, Hoteit I. 2023. Long-term variability in the Arabian Peninsula droughts driven by the Atlantic multidecadal oscillation. Earth's Future **11**, e2023EF003549.

Samuilov S, Lang F, Djukic M, Djunisijevic-Bojovic D, Rennenberg H. 2016. Lead uptake increases drought tolerance of wild type and transgenic poplar (*Populus tremula* × *P. alba*) overexpressing gsh 1. Environmental Pollution **216**, 773–785.

Schupp R, Rennenberg H. 1988. Diurnal changes in the glutathione content of spruce needles (*Picea abies* L.). Plant Science **57**, 113–117.

Shabala S. 2013. Learning from halophytes: physiological basis and strategies to improve abiotic stress tolerance in crops. Annals of Botany **112**, 1209–1221.

Shabala S, Shabala L. 2011. Ion transport and osmotic adjustment in plants and bacteria. Biomolecular Concepts **2**, 407–419.

Shannon P, Markiel A, Ozier O, Baliga NS, Wang JT, Ramage D, Amin N, Schwikowski B, Ideker T. 2003. Cytoscape: a software environment for integrated models of biomolecular int4eraction networks. Genome Research **13**, 2498–2504.

Shareef HJ, Abdi G, Fahad S. 2020. Change in photosynthetic pigments of date palm offshoots under abiotic stress factors. Folia Oecologica **47**, 45–51.

Sharma P, Lakra N, Goyal A, Ahlawat YK, Zaid A, Siddique KHM. 2023. Drought and heat stress mediated activation of lipid signaling in plants: a critical review. Frontiers in Plant Science **14**, 1216835.

Singh G, Dhar YV, Asif MH, Misra P. 2018. Exploring the functional significance of sterol glycosyltransferase enzymes. Progress in Lipid Research **69**, 1–10.

Slama I, Abdelly C, Bouchereau A, Flowers T, Savouré A. 2015. Diversity, distribution and roles of osmoprotective compounds accumulated in halophytes under abiotic stress. Annals of Botany **115**, 433–447.

Soares ALC, Geilfus C-M, Carpentier SC. 2018. Genotype-specific growth and proteomic responses of maize toward salt stress. Frontiers in Plant Science **9**, 661.

Sreenivasulu N, Harshavardhan VT, Govind G, Seiler C, Kohli A. 2012. Contrapuntal role of ABA: does it mediate stress tolerance or plant growth retardation under long-term drought stress? Gene **506**, 265–273.

Strohm M, Jouanin L, Kunert KJ, Pruvost C, Polle A, Foyer CH, Rennenberg H. 1995. Regulation of glutathione synthesis in leaves of transgenic poplar (*Populus tremula* × *P. alba*) overexpressing glutathione synthetase. The Plant Journal **7**, 141–145.

Tabari H, Willems P. 2018. More prolonged droughts by the end of the century in the Middle East. Environmental Research Letters **13**, 104005.

Vadassery J, Reichelt M, Hause B, Gershenzon J, Boland W, Mithöfer A. 2012. CML42-mediated calcium signaling coordinates responses to Spodoptera herbivory and abiotic stresses in Arabidopsis. Plant Physiology **159**, 1159–1175.

van Wesemael J, Hueber Y, Kissel E, Campos N, Swennen R, Carpentier S. 2018. Homeolog expression analysis in an allotriploid non-model crop via integration of transcriptomics and proteomics. Scientific Reports **8**, 1353.

Velikova V, Yordanov I, Edreva A. 2000. Oxidative stress and some antioxidant systems in acid rain-treated bean plants. Plant Science **151**, 59–66.

Verslues PE, Agarwal M, Katiyar-Agarwal S, Zhu J, Zhu J-K. 2006. Methods and concepts in quantifying resistance to drought, salt and freezing, abiotic stresses that affect plant water status. The Plant Journal **45**, 523–539.

White PJ, Broadley MR, Thompson JA, McNicol JW, Crawley MJ, Poulton PR, Johnston AE. 2012. Testing the distinctness of shoot ionomes of angiosperm families using the Rothamsted Park grass continuous hay experiment. New Phytologist **196**, 101–109.

Wickham H. 2016. Getting started with ggplot2. In: ggplot2: elegant graphics for data analysis. Cham: Springer, 11–31.

Xu Y-H, Liu R, Yan L, Liu Z-Q, Jiang S-C, Shen Y-Y, Wang X-F, Zhang D-P. 2012. Light-harvesting chlorophyll a/b-binding proteins are required for stomatal response to abscisic acid in Arabidopsis. Journal of Experimental Botany **63**, 1095–1106.

Yaish MW. 2015. Proline accumulation is a general response to abiotic stress in the date palm tree (*Phoenix dactylifera* L.). Genetics and Molecular Research **14**, 9943–9950.

Yaish MW, Kumar PP. 2015. Salt tolerance research in date palm tree (*Phoenix dactylifera* L.), past, present, and future perspectives. Frontiers in Plant Science **6**, 348.

Yao C, Finlayson SA. 2015. Abscisic acid is a general negative regulator of Arabidopsis axillary bud growth. Plant Physiology **169**, 611–626.

Yeo AR. 1983. Salinity resistance: physiologies and prices. Physiologia Plantarum **58**, 214–222.

Yoshida T, Mogami J, Yamaguchi-Shinozaki K. 2014. ABA-dependent and ABA-independent signaling in response to osmotic stress in plants. Current Opinion in Plant Biology **21**, 133–139.

Young DY, Pang N, Shachar-Hill Y. 2022. 13C-labeling reveals how membrane lipid components contribute to triacylglycerol accumulation in Chlamydomonas. Plant Physiology **189**, 1326–1344.

Yu L, Zhou C, Fan J, Shanklin J, Xu C. 2021. Mechanisms and functions of membrane lipid remodeling in plants. The Plant Journal **107**, 37–53.

Zolla L, Rinalducci S. 2002. Involvement of active oxygen species in degradation of light-harvesting proteins under light stresses. Biochemistry **41**, 14391–14402.